PNAS

Supporting Information for

Bimodular Architecture of Bacterial Effector SAP05 that Drives Ubiquitin-Independent Targeted Protein Degradation

Qun Liu[a,1], Abbas Maqbool[b,c,1], Federico G. Mirkin[a], Yeshveer Singh[a], Clare E. M. Stevenson[b], David M. Lawson[b], Sophien Kamoun[c], Weijie Huang[d,*] and Saskia A. Hogenhout[a,*]

[a] Department of Crop Genetics, John Innes Centre, Norwich Research Park, Norwich NR4 7UH, United Kingdom; [b] Department of Biochemistry and Metabolism, John Innes Centre, Norwich Research Park, Norwich NR4 7UH, United Kingdom; [c] The Sainsbury Laboratory, University of East Anglia, Norwich NR4 7UH, United Kingdom; [d] National Key Laboratory of Plant Molecular Genetics, Shanghai Centre for Plant Stress Biology, Centre for Excellence in Molecular Plant Sciences, Chinese Academy of Sciences, Shanghai, China.

This SI Appendix includes:

[1]These authors contributed equally to the work.

*To whom correspondence may be addressed. Email: wjhuang@cemps.ac.cn or saskia.hogenhout@jic.ac.uk.

Materials and Methods

Gene cloning, expression, and protein purification for crystallization and *in vitro* studies

For crystallization of SAP05 – $SPL5^{ZnF}$ complex, DNA encoding mature SAP05 excluding signal peptide (Ala33-Lys135) and DNA encoding the ZnF domain of SPL5 (Ser60-Leu127) were separately subcloned to pOPINF vector for N-terminal 6×His tags (1) using In-fusion cloning method (2, 3). The constructs were transformed individually into *E. coli* BL21 (DE3) competent cells. Bacterial cultures were grown in LB media (containing 50 µg/mL ampicillin) at 37 °C to an OD_{600} around 0.5 followed by induction with 1 mM Isopropyl-b-D-thiogalactoside (IPTG) at 16 °C overnight with shaking at a speed of 220 rpm. Cell pellets were resuspended in buffer A1 (50 mM Tris-HCl, 50 mM glycine, 0.5 M NaCl, 20 mM imidazole, 5% glycerol, pH 8.0) followed by sonication lysis at 40% amplitude, 5 sec on / 10 sec off pulse for 30 min on ice. Cell debris was removed by centrifuge at 20000 g for 20 min. Purification of the proteins was performed using an ÄKTA Xpress purification system comprising initial capture with metal affinity chromatography (IMAC) using Ni-NTA column, which elutes proteins with buffer B1 (50 mM Tris-HCl, 50 mM glycine, 0.5 M NaCl, 0.5 M imidazole, 5% glycerol, pH 8.0), followed by gel filtration with the column Superdex 75 26/600 in buffer A4 (20 mM HEPES, 0.15 M NaCl, pH 7.5). Fractions with the elution peaks were assessed by SDS-PAGE gels, pooled and treated with HRV-3C protease overnight at 4°C. Afterwards, digested protein samples were passed through Ni-NTA column to remove cleaved 6×His tags. Untagged samples were assessed with SDS-PAGE gels, pooled and concentrated with 3 kDa cut-off vivaspin concentrators, followed by a second round of gel filtration with Superdex 75 26/600 in buffer A4. Eluted samples were assessed with SDS-PAGE gels. Afterwards, purified proteins were mixed together in equimolar ratio, followed by gel filtration chromatography. Eluted fractions were assessed by SDS-PAGE, pooled and concentrated to a final concentration of 15 mg/mL, for crystallization studies.

For crystallization of SAP05 – $Rpn10^{vWA}$ complex, the mature coding sequence of SAP05 (Ala33-Lys135) was cloned to pOPINF vector, $Rpn10^{vWA}$ (Val2-GLy193) was initially

cloned to pOPINM to make MBP-vWA fusion cassette. MBP-vWA was then amplified and ligated to pOPINA to remove the 6×His tag. The final constructs were co-transformed into *E. coli* BL21(DE3) competent cells. Proteins were co-expressed and co-purified using the IMAC and gel filtration as mentioned above. Eluted fractions from the complex were assessed from gel filtration peaks and SDS-PAGE. Afterwards, the eluted complex was subjected to HRV-3C protease cleavage overnight at 4°C followed by Ni-NTA column to remove tags. After a second round of gel filtration followed by assessment with SDS-PAGE, the purified complexes were pooled and concentrated to 15 mg/mL for crystallization studies.

For *in vitro* experiments, purified proteins were concentrated to ~10 mg/mL via 3 kDa cut-off vivaspin concentrators for subsequent analysis. Detection of proteins on SDS-PAGE gels was performed using Instant Blue staining solution (Abcam). Data of gel filtration traces were processed and plotted using ggplot2 in R (4).

Protein crystallization, structure determination, and refinement

Crystallization screens were set up in sitting-drop vapor diffusion format in MRC2 96-well crystallization plates with drops comprised of 0.3 µL precipitant solution and 0.3 µL of protein and incubated at 293 K. All crystals were cryoprotected in the crystallization solution supplemented with 25% (v/v) glycerol and mounted in Litholoops (Molecular Dimensions) before flash-cooling by plunging into liquid nitrogen. X-ray data were recorded on beamline I04 at the Diamond Light Source (Oxfordshire, UK) using an Eiger2 XE 16M hybrid photon counting detector (Dectris), with crystals maintained at 100 K by a Cryojet cryocooler (Oxford Instruments). Diffraction data were integrated and scaled using DIALS (5) via the XIA2 expert system (6), then merged using AIMLESS (7). The majority of the downstream analysis was performed through the CCP4i2 graphical user interface (8). Data collection statistics are summarized in Table 1.

The SAP05 – $SPL5^{ZnF}$ complex crystallized from 0.1 M MES pH 6.5, 25% (w/v) PEG 6000 in space group $P2_1$, with approximate cell parameters of a = 78.7, b = 165.0, c = 80.9 Å, β = 109.7°. All X-ray data were collected from a single crystal, initially recorded at

a wavelength of 0.9795 Å (2 x 360° passes) and processed to 2.2 Å resolution, and then at a wavelength of 1.2770 Å (1 x 360° pass), this being close to the *K* X-ray absorption edge for zinc. The latter data set was processed to 2.4 Å resolution and enabled structure solution via the single-wavelength anomalous diffraction method using the CRANK2 pipeline (9), due to the presence of Zn^{2+} ions bound to $SPL5^{ZnF}$. This produced a partial model corresponding to eight copies of a 1:1 complex of SAP05 – $SPL5^{ZnF}$ in the crystallographic asymmetric unit, giving an estimated solvent content of 59%, with each copy of $SPL5^{ZnF}$ containing two Zn^{2+} ions. The model was completed through several iterations of model building in COOT (10) and restrained refinement in REFMAC5 (11) against the higher resolution data set at 2.2 Å resolution. Refinement and validation statistics are summarized in Table 1.

The SAP05 – $Rpn10^{vWA}$ complex crystallized from 0.1 M Sodium HEPES pH 7.5, 10.7 % (w/v) PEG 4000 in space group $P2_1$, with approximate cell parameters of a = 42.4, b = 68.6, c = 49.9 Å, β = 92.8°. X-ray data were recorded from a single crystal at a wavelength of 0.9796 Å (2 x 360° passes) and processed to 2.17 Å resolution. Analysis of the likely composition of the asymmetric unit suggested that it contained one copy of a 1:1 complex of SAP05 – $Rpn10^{vWA}$, giving an estimated solvent content of 44%. The structure was solved via molecular replacement using PHASER (12). One copy of SAP05 was taken from the above SAP05 – $SPL5^{ZnF}$ complex as the first template, and the second template was derived from a homology model of $Rpn10^{vWA}$ produced by Swiss-Model (13) and based on PDB entry 5VFT (14). The model was completed through several iterations of model building in COOT and restrained refinement in REFMAC5. Refinement and validation statistics are summarized in Table 1. All structural figures were prepared using CCP4mg (15). Distances between residues were measured with COOT (10).

Yeast two-hybrid assay (Y2H)

The coding sequences of SAP05 or SAP05 mutants excluding signal peptides were amplified and ligated into Gateway vector pDEST-GBKT7 (BD). Full length sequences of *A. thaliana* Rpn10, two SPLs (SPL11 and SPL15), and three GATAs (GATA18, GATA19 and GATA25) were amplified and cloned into vector pDEST-GADKT7 (AD) using

Gateway cloning methods (16, 17). Constructs used to test protein-protein interactions were co-transformed into the yeast *Saccharomyces cerevisiae* strain AH109 using the Matchmaker Gold yeast two-hybrid system (Clontech). Empty pDEST-GBKT7 and pDEST-GADKT7 vectors were used as negative control. Yeast growth was assessed on solid double dropout medium lacking leucine and tryptophan (SD-LW) which indicates the presence of both AD and BD constructs. Interactions between AD and BD fusion proteins were screened on selective dropout medium; triple dropout medium lacking leucine, tryptophan and histidine (SD-LWH) or with the addition of 3-amino-1,2,4-triazole (3-AT) at a final concentration of 10 mM when self-activation was observed or to improve selection stringency, and quadruple dropout medium lacking leucine, tryptophan, histidine and adenine (SD-LWHA). Yeast plates were kept in 28°C incubators for 5 days before imaging.

Degradation assay in *N. benthamiana*

The coding sequences of SAP05 or SAP05 mutants (excluding signal peptides) were amplified and ligated into Gateway vector pB7WG2. Full length coding sequence of AtSPL5 were amplified and tagged with 3×HA at N-terminal, then ligated into Gateway vector pB7WG2. After sequencing, the constructs were separately transformed to *Agrobacterium tumefaciens* strain GV3101 and plated on LB solid medium containing rifampicin, gentamicin and spectinomycin and grown at 28 °C for 24-48 h. Then colonies were picked and checked by PCR using plasmids extracted from overnight liquid culture and gene-specific primers. Positive colonies were grown at 28 °C overnight, harvested, and resuspended in infiltration buffer (10 mM $MgCl_2$, 10 mM MES, pH 5.6), supplemented with 100 μM acetosyringone. Appropriate combinations of above constructs together with pCB301-P19 were mixed at an OD_{600} of 0.5 per construct and infiltrated to the abaxial surface of 4-week-old *N. benthamiana* leaves using 1 ml needleless syringe. Infiltrations were conducted on randomly selected leaves, with triplicates consisting of three leaves each. To minimize variation, each single leaf was infiltrated with four combinations: SAP05 only, one SAP05 mutant only, SAP05 plus HA-SPL5, and SAP05 mutant plus HA-SPL5. After 3 days post-infiltration, the infiltrated leaves were detached, and the infiltrated areas were harvested for total protein extraction.

To detect SPL5 and SAP05, western blots were performed as follows. Total protein extracts were separated on 4-20% gradient gels (Bio-Rad) and transferred to 0.22 µm PVDF membranes using the Bio-Rad mini-PROTEAN Electrophoresis system. Protein loading was visualized with Ponceau S staining solution (Thermo Scientific) and washed off with water. Membranes were then blocked by 5% (w/v) milk powder in Tris-buffered saline (TBS) and 0.1% (v/v) Tween-20 for 2 h at room temperature. Membranes were then overnight incubated at 4°C with the anti-HA primary antibody (OptimAb HA. 11, Eurogentec), which was raised from mouse serum, at a ratio of 1:2000 dilution. Afterwards, the membrane was probed with Alkaline-Phosphatase-conjugated anti-mouse secondary antibody (Thermo Scientific) for 1 h at room temperature and imaged after incubation with NBT/BCIP substrate solution (Thermo Scientific). Membranes were washed after detection, blocked in the same conditions as previously described and incubated overnight at 4°C with rabbit raised anti-SAP05 antibody at a 1:5000 ratio (18). The membrane was then probed with HRP conjugated anti-rabbit secondary antibody (Sigma) and imaged with Immobilon Western Chemiluminescent HRP Substrate (Sigma).

Degradation assay in *A. thaliana* protoplast

A. thaliana (Col-0) mesophyll protoplast isolation and transformation were carried out as previously reported (19). Briefly, protoplasts from the mesophyll cells were isolated from leaves of 3-4 week-old plants which were grown under short-day (10 h light/14 h dark) conditions at 22°C. For transfection, 300 µL of fresh protoplast solution (400,000/mL) was co-transformed with 12 µg high quality plasmids for each construct using PEG-calcium method. Transfected protoplasts were incubated at 22°C for 16 h in dark. Following which, total protein was extracted and examined via western blots using HRP-conjugated anti-mouse secondary antibody (Sigma). Protein loading was visualized with Amido Black Staining Solution (Sigma).

A

SAP05 (12.3 kDa):

MFKIKNNLLKSKIFVFILLGLFVIINNHQAMAAPNEEFVGDMRIVNVNLSNIDILKKHETFKKYFDFTLTGPRYNGNIAEFAMI
WKIKNPPLNLLGVFFDDGTRDDEDDKYILEELKQIGNGAKNMYIFWQYEQK

SPL5^{ZnF} (8.1 kDa):

MEGQRTQRRGYLKDKATVSNLVEEEMENGMDGEEEDGGDEDKRKKVMERVRGPSTDRVPSRLCQVDRCTVNLTEAK
QYYRRHRVCEVHAKASAATVAGVRQRFCQQCSRFHELPEFDEAKRSCRRRLAGHNERRRKISGDSFGEGSGRRGFS
GQLIQTQERNRVDRKLPMTNSSFKRPQIR

Rpn10^{vWA} (20.7 kDa):

MVLEATMICIDNSEWMRNGDYSPSRLQAQTEAVNLLCGAKTQSNPENTVGILTMAGKGVRVLTTPTSDLGKILACMHGL
DVGGEINLTAAIQIAQLALKHRQNKNQRQRIIVFAGSPIKYEKKALEIVGKRLKKNSVSLDIVNFGEDDDEEKPQKLEALLTA
VNNNDGSHIVHVPSGANALSDVLLSTPVFTGDEGASGYVSAAAAAAAAGGDFDFGVDPNIDPELALALRVSMEEERARQ
EAAAKKAADEAGQKDKDGDTASASQETVARTTDKNAEPMDEDSALLDQAIAMSVGDVNMSEAADEDQDLALALQMSM
SGEESSEATGAGNNLLGNQAFISSVLSSLPGVDPNDPAVKELLASLPDESKRTEEEESSSKKGEDEKK

B

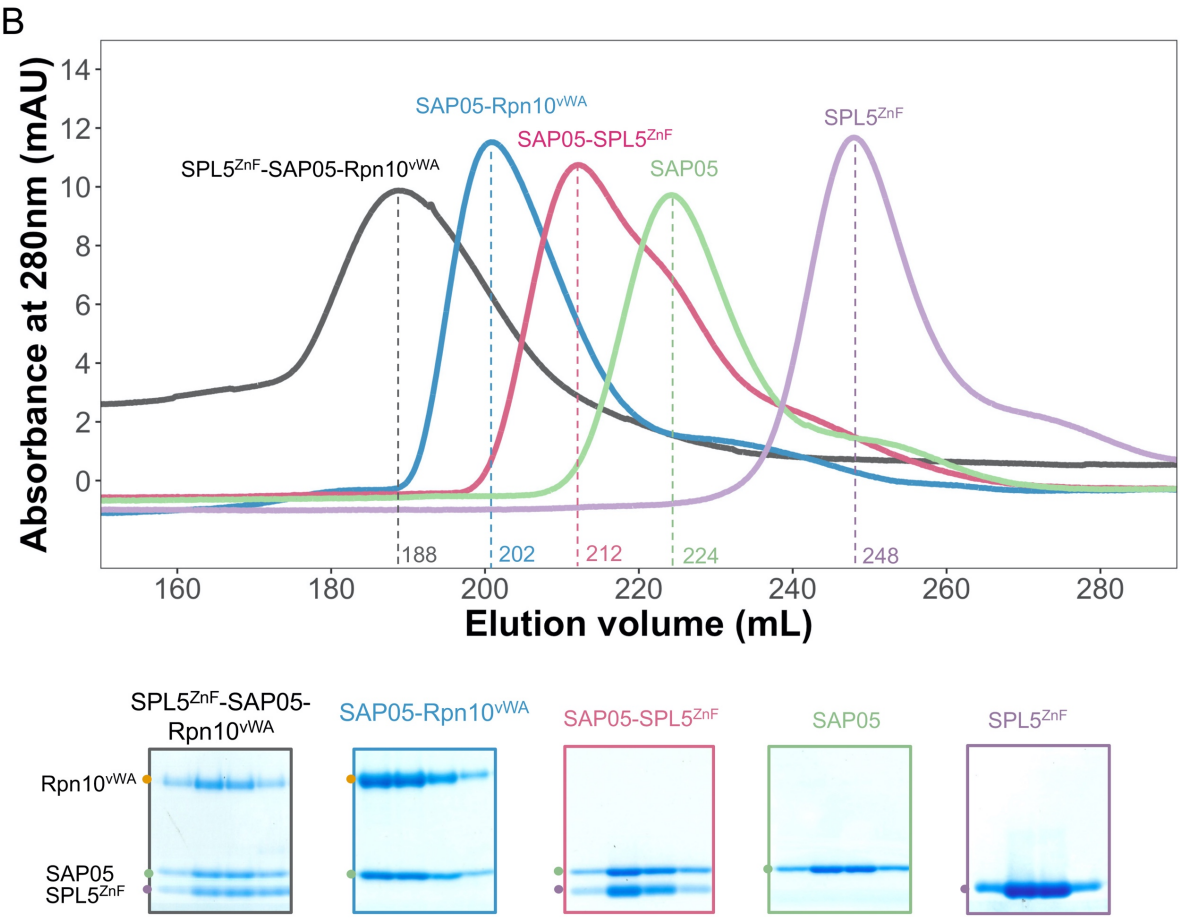

Fig. S1. Expression and purification of SAP05 – SPL5^{ZnF} and SAP05 – Rpn10^{vWA} complexes for crystallization. (A) The amino acid sequences of mature SAP05, SPL5^{ZnF}, and Rpn10^{vWA} utilized for protein expression are highlighted in yellow on full-length proteins and their molecular weights are indicated in brackets. (B) Gel filtration chromatogram (top) and SDS-PAGE (bottom) analyses of peak fractions of purified

SAP05, SPL5^{ZnF}, SAP05 – SPL5^{ZnF}, SAP05 – Rpn10^{vWA} and SPL5^{ZnF} – SAP05 – Rpn10^{vWA} complexes. SDS-PAGE gels are framed with the same color as the corresponding elution peak in gel filtration chromatogram. Yellow, green and purple dots indicate the expected size of Rpn10^{vWA}, SAP05 and SPL5^{ZnF}, respectively.

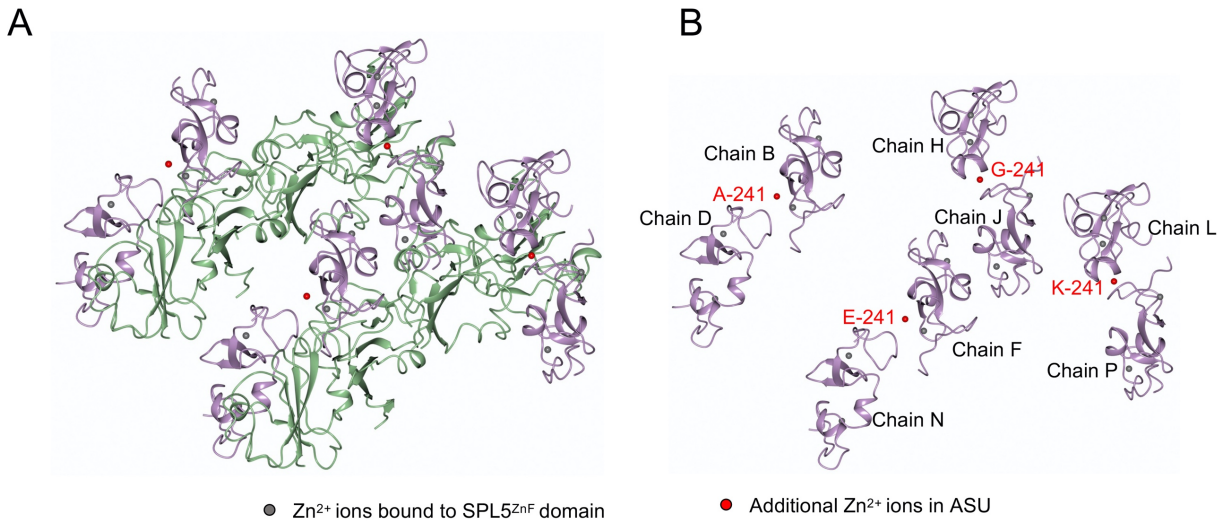

Fig. S2. Position of Zn^{2+} ions in asymmetric unit (ASU) in the SAP05 – $SPL5^{ZnF}$ crystal. (A) Eight copies of SAP05 – $SPL5^{ZnF}$ complex in ASU are shown as cartoon (SAP05 colored green and $SPL5^{ZnF}$ colored purple). (B) Eight copies of $SPL5^{ZnF}$ in ASU are shown as cartoon (purple). The chain IDs are labelled. Structural Zn^{2+} ions within each $SPL5^{ZnF}$ domain are shown as grey spheres, and four additional Zn^{2+} ions are shown as red spheres.

A

SAP05 and SPL5^{ZnF} interface

Residues on SAP05	Residues on SPL5^{ZnF}	Mutated residues on SAP05
D66	Q77	D66A, D66E
G76	Q105	G76W
N77	Y78, Q105, S108	N77A, N77D, N77R
E80	R81	E80A, E80R
R104	Q105	-
D106	K90, R121	D106A, D106R

B

SAP05 and Rpn10^{vWA} interface

Residues on SAP05	Residues on Rpn10^{vWA}	Mutated residues on SAP05
R43	D68	R43A, R43E
N48	Q27	-
S50	E31	S50A
H58	N34	H58A, H58W
T60	G38, Q42	T60W
N125	D68	N125A, N125D
Y127	G70	Y127W
Y132*	S24*	-

Fig. S3. Residues on SAP05 – SPL5^{ZnF} and SAP05 – Rpn10^{vWA} interfaces and the mutations generated on SAP05. Interacting residues and generated SAP05 mutations on SAP05 – SPL5^{ZnF} (A) and SAP05 – Rpn10^{vWA} (B) interaction interface. Interactions were analyzed with CCP4mg. *The electron density for Rpn10^{vWA} S24 is suboptimal, implying uncertainty regarding its precise placement and proximity for its potential interaction with SAP05 Y132.

A

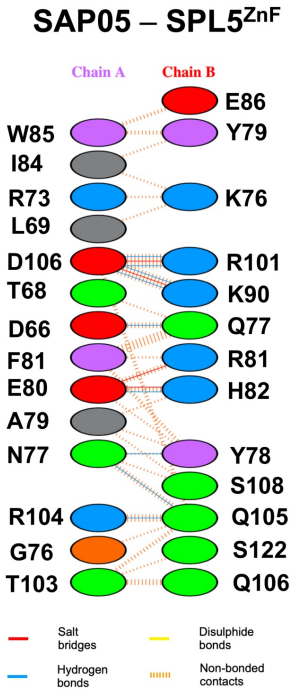

B

Distance of some interacting residues between SAP05 and SPL5^{ZnF}

Residues on SAP05	Residues on SPL5^{ZnF}	Distance (Å)
D66	Q77	2.67
G76	Q105	3.53
N77	Y78	3.07
N77	Q105	2.76
N77	S108	3.13
E80	R81	2.86, 3.23
R104	Q105	2.63
D106	K90	2.73
D106	R121	2.80, 2.83

C

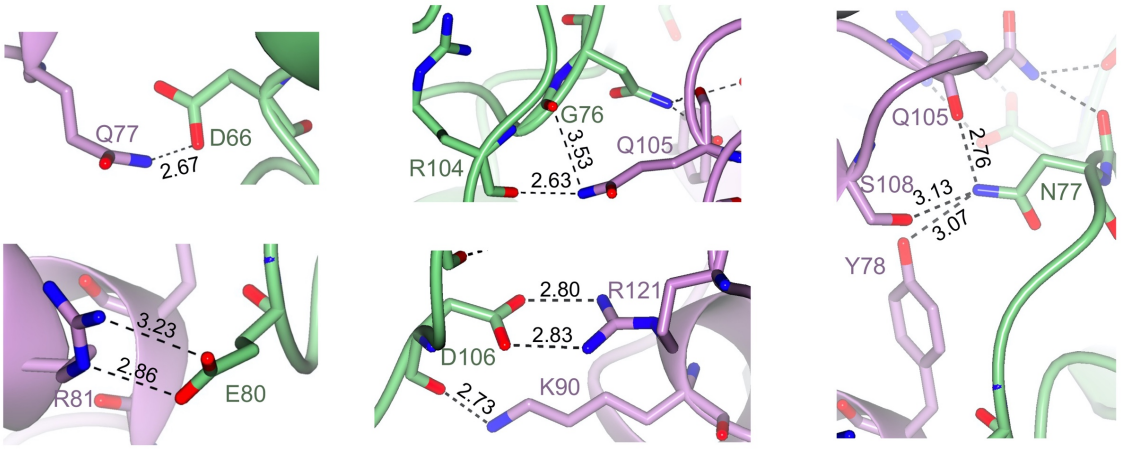

Fig. S4. Analysis of interacting residues on SAP05 – SPL5^{ZnF} interface. (A) Different types of interaction between residues on SAP05 and SPL5^{ZnF} by PDBsum (https://www.ebi.ac.uk/thornton-srv/databases/cgi-bin/pdbsum/GetPage.pl?pdbcode=8pfc&template=interfaces.html&o=RESIDUE&l=1). (B) Distances of important interacting residues measured with Coot. (C) Distances between of interacting residues shown in SAP05 – SPL5^{ZnF} structure.

Cell		Syringe		T (°C)	N	K_d (M^{-6})	ΔH (kcal·mol^{-1})	ΔG (kcal·mol^{-1})
Contents	Conc. (μM)	Contents	Conc. (μM)					
SPL5^{ZnF}	20	SAP05	200	25	1.15	0.510	-14.4 ± 0.919	-8.59
SPL5^{ZnF}	20	SAP05	200	25	1.05	0.388	-11.9 ± 1.29	-8.57
SPL5^{ZnF}	20	SAP05	200	25	1.01	0.445	-18.1 ± 1.45	-8.67
SAP05	20	SPL5^{ZnF}	250	25	0.942	0.458	-14.9 ± 0.998	-8.65
SAP05	20	SPL5^{ZnF}	250	25	0.835	0.560	-14.3 ± 0.435	-8.53
SAP05	20	SPL5^{ZnF}	250	25	0.914	0.541	-14.3 ± 0.425	-8.55
SAP05-Rpn10^{vWA}	20	SPL5^{ZnF}	200	25	0.995	0.683	-10.8 ± 0.164	-8.41
SAP05-Rpn10^{vWA}	20	SPL5^{ZnF}	200	25	1.06	0.620	-7.87 ± 0.754	-8.47
SAP05^{D66A}	20	SPL5^{ZnF}	200	25	n.b.	n.b.	n.b.	n.b.
SAP05^{D66A}	20	SPL5^{ZnF}	200	25	n.b.	n.b.	n.b.	n.b.
SAP05^{D66A}	20	SPL5^{ZnF}	200	25	n.b.	n.b.	n.b.	n.b.
SAP05^{D66E}	30	SPL5^{ZnF}	500	25	1.11	15.8	-7.32 ± 3.62	-6.55
SAP05^{D66E}	30	SPL5^{ZnF}	500	25	1.22	19.6	-7.30 ± 1.74	-6.42
SAP05^{N77R}	20	SPL5^{ZnF}	200	25	n.b.	n.b.	n.b.	n.b.
SAP05^{N77R}	20	SPL5^{ZnF}	200	25	n.b.	n.b.	n.b.	n.b.
SAP05^{N77R}	20	SPL5^{ZnF}	200	25	n.b.	n.b.	n.b.	n.b.
SAP05$^{H58A-T60W}$	20	SPL5^{ZnF}	300	25	0.967	2.69	-5.63 ± 0.173	-7.60
SAP05$^{H58A-T60W}$	20	SPL5^{ZnF}	300	25	1.00	4.247	-6.18 ± 0.338	-7.33
SAP05$^{H58A-T60W}$	20	SPL5^{ZnF}	300	25	1.08	3.85	-5.76 ± 0.201	-7.39

Fig. S5. Thermodynamic parameters obtained from ITC binding experiments. Two or three repeats of ITC tests by titrating SAP05 to SPL5^{ZnF} or SPL5^{ZnF} to SAP05-Rpn10^{vWA} complex or different SAP05 mutants. Conc., concentration. n.b., not binding.

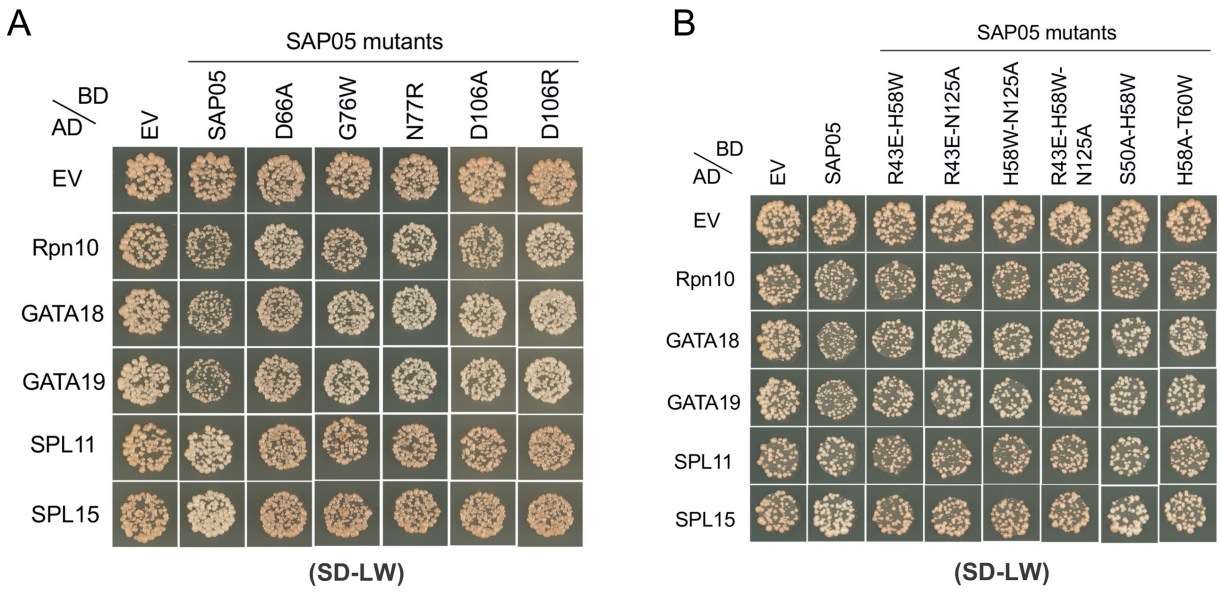

Fig. S6. Yeast transformation controls for Y2H assays in the study, related to Figures 2 and 3. (A) Yeast growth on double dropout medium lacking leucine and tryptophan indicating the expression of AD and BD constructs in Y2H assays for Figure 2E (A) and Figure 3C (B) in the main text.

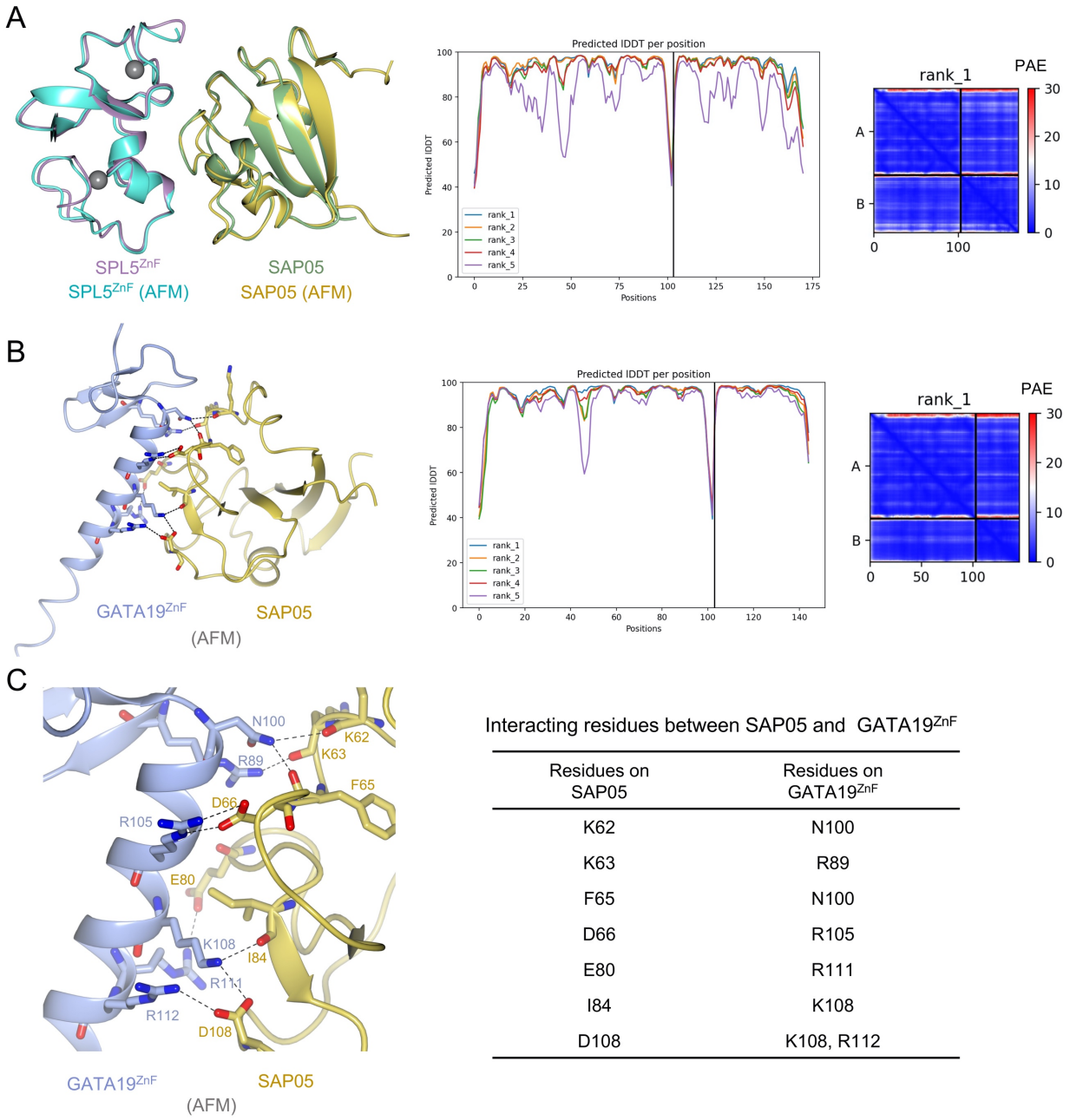

Interacting residues between SAP05 and GATA19^{ZnF}

Residues on SAP05	Residues on GATA19^{ZnF}
K62	N100
K63	R89
F65	N100
D66	R105
E80	R111
I84	K108
D108	K108, R112

Fig. S7. Structural prediction of SAP05 – SPL5^{ZnF} and SAP05 – GATA19^{ZnF} complexes. (A) Left, AlphaFold model (AFM) for SAP05 – SPL5^{ZnF} complex (yellow – cyan) superimposed on the crystal structure of SAP05 – SPL5^{ZnF} complex (green – purple). Middle, the predicted local Distance Difference Test (lDDT) value of SAP05 – SPL5^{ZnF} model, showing the quality of predicted models by evaluating local distance differences to the reference. Best model (rank_1) was used for superimposition. Right, predicted aligned error (PAE) of the rank_1 model, showing the estimate of position error

between predicted and true structures. Blue means lower error scores, red means higher error scores. (B) Left, AFM model (rank_1) of SAP05 – GATA19^{ZnF} complex (yellow – light blue). Middle, predicted lDDT value of SAP05 – GATA19^{ZnF} complex. Right, predicted aligned error (PAE) of the rank_1 model. (C) Left, enlarged view for predicted SAP05 – GATA19^{ZnF} interaction interface. SAP05 residues and GATA19^{ZnF} residues that involved for interaction with GATA19^{ZnF} were labelled in yellow and light blue, respectively. Dashed line shows predicted interactions between SAP05 and GATA19^{ZnF} from AFM model. Right, interacting residues between SAP05 and GATA19^{ZnF} of predicted structure.

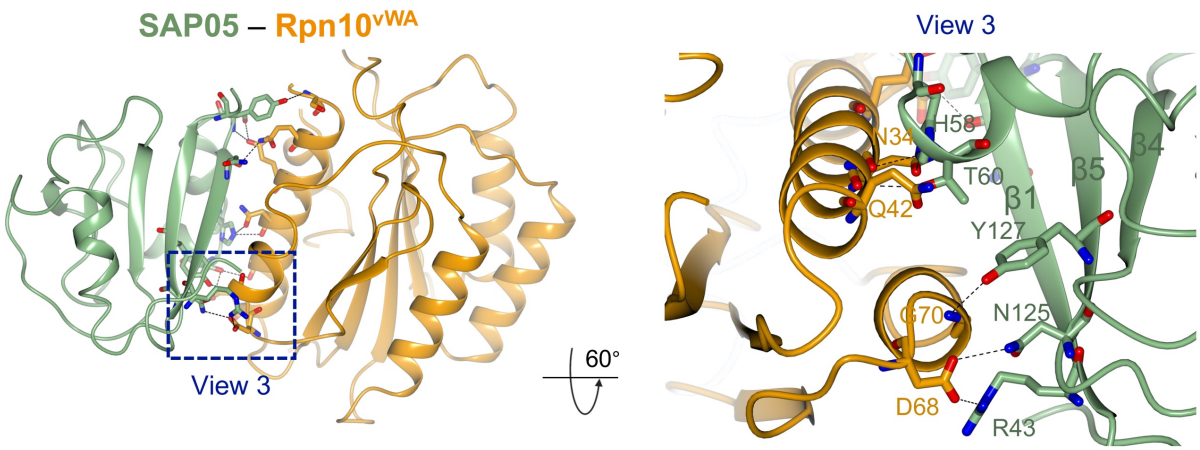

Fig. S8. Another view of SAP05 – Rpn10^{vWA} interaction. Left, the overview of the interacting interface with the dashed square displaying the areas for enlarged view. Right, the enlarged and rotated view 3 of the lower part of the interface.

A

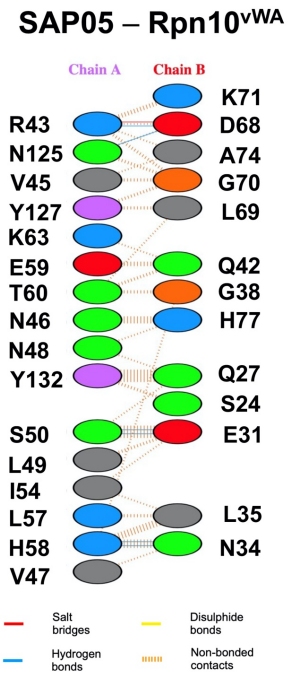

B

Distance of some interacting residues between SAP05 and Rpn10^{vWA}

Residues on SAP05	Residues on Rpn10^{vWA}	Distance (Å)
R43	D68	3.10
N48	Q27	3.54
S50	E31	2.48, 2.57
H58	N34	2.86, 3.08
T60	G38	3.76
T60	Q42	3.67
N125	D68	3.23
Y127	G70	3.26
Y132*	S24*	3.58*

C

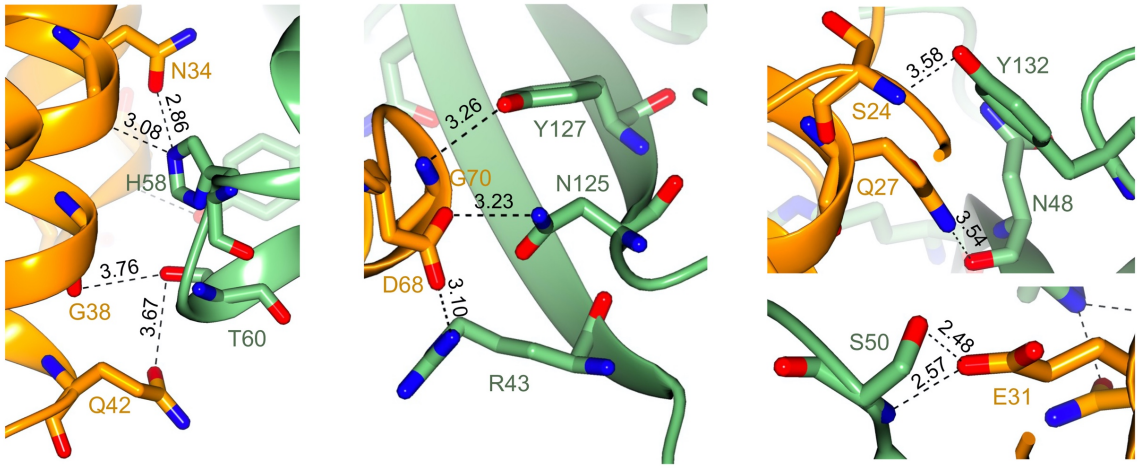

Fig. S9. Analysis of interacting residues on SAP05 – Rpn10^{vWA} interface. (A) Different types of interaction between residues on SAP05 and Rpn10^{vWA} by PDBsum (https://www.ebi.ac.uk/thornton-srv/databases/cgi-bin/pdbsum/GetPage.pl?pdbcode=8pfd&template=interfaces.html&o=RESIDUE&l=1). (B) Distances of important interacting residues measured with Coot. (C) Distances between interacting residues shown on SAP05-Rpn10^{vWA} structure. *The electron density for Rpn10^{vWA} S24 is suboptimal, implying uncertainty regarding its precise placement and proximity for its potential interaction with SAP05 Y132..

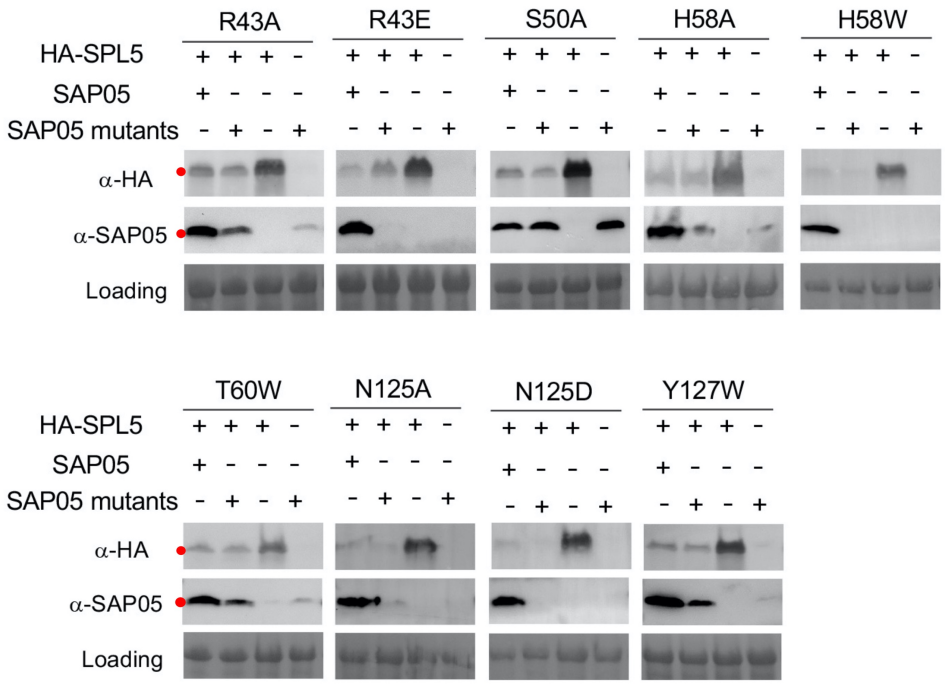

Fig. S10. Western blot analysis of proteasomal degradation of SPL5 in presence of SAP05 wild-type or single mutants on sheet surface. Red dots on the blots indicate the expected sizes of the transiently expressed proteins in *N. benthamiana* leaves. Protein loading was visualized using Ponceau S staining. HA, Hemagglutinin.

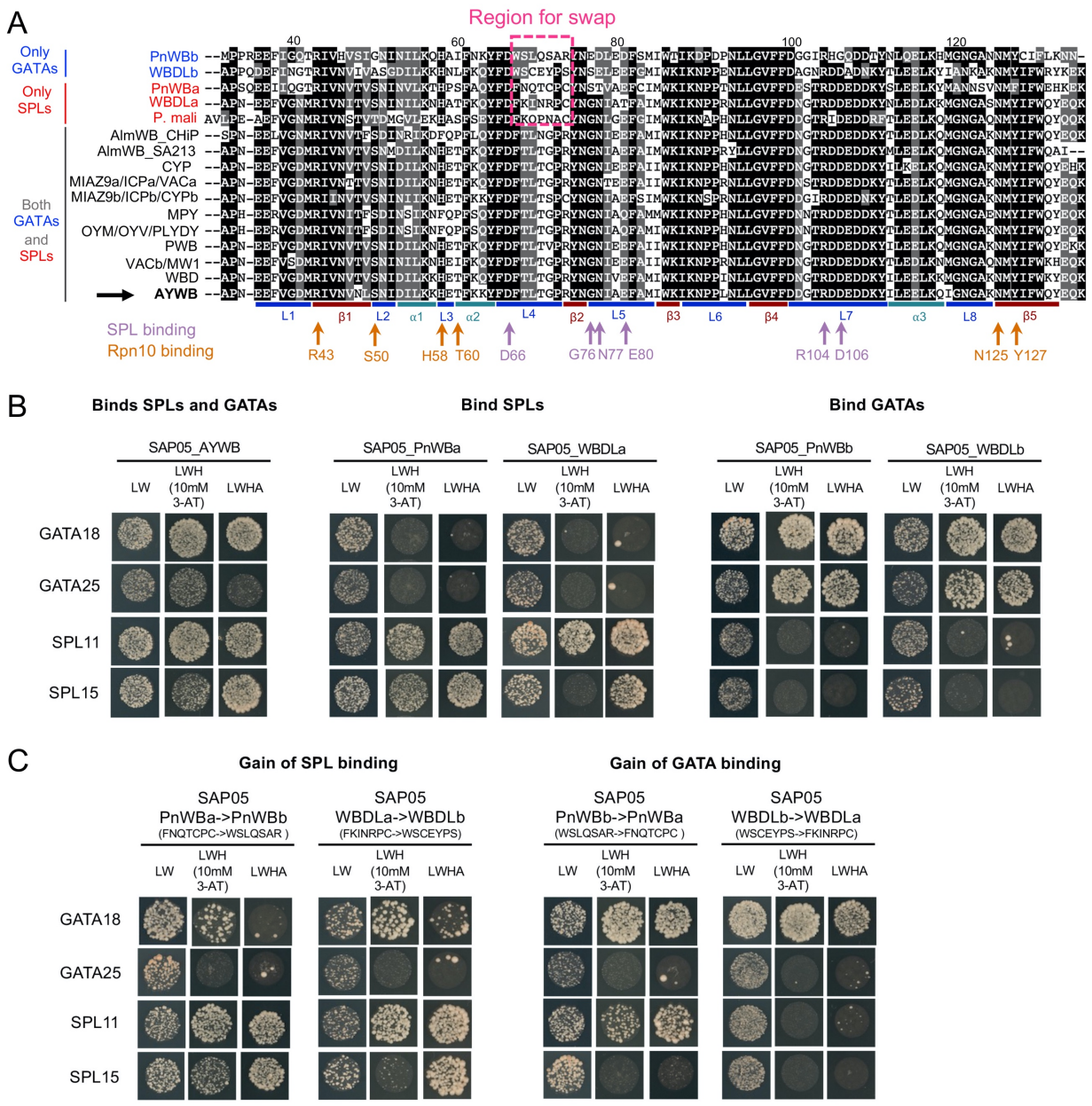

Fig. S11. Conservation of SPL, GATA and Rpn10-interacting residues in SAP05 homologs. (A) Multiple sequence alignment of SAP05 homologs from different phytoplasma species showing that the Rpn10-binding or SPL binding residues are well conserved. Identical and conserved amino acid residues are denoted by black and gray backgrounds, respectively. Homologs binding only GATAs, only SPLs, and both GATAs and SPLs are displayed in blue, red and black, respectively. The secondary structure of AYWB SAP05 is highlighted at the bottom. SAP05 residues involved in SPL binding (purple) or Rpn10 binding (orange) are pointed with arrows. The region used for swap in

(C) is marked with pink dashed rectangle. (B) Y2H assay showing SAP05 homologs that specifically bind SPLs or GATAs. (C) Y2H assay showing that swapping loop 4 sequences from GATA-binding SAP05 homologs contributes to SPL binding, and swapping loop 4 sequences from SPL-binding SAP05 homologs leads to GATA binding.

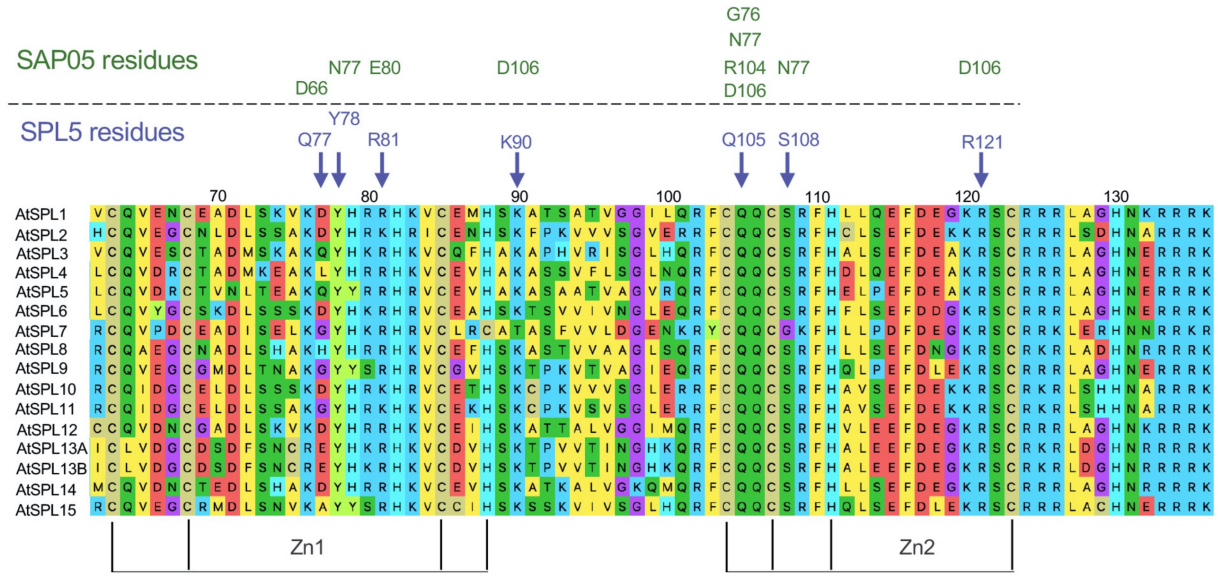

Fig. S12. Multiple sequence alignment of ZnF domains of *A. thaliana* SPLs using MUSCLE. The conserved SPL residues involved in the interaction with SAP05 are indicated with purple arrows and the corresponding SAP05 residues are shown in green. Accession numbers for AtSPLs are: SPL1, AT2G47070; SPL2, AT5G43270; SPL3, AT2G33810; SPL4, AT1G53160; SPL5, AT3G15270; SPL6, AT1G69170; SPL7, AT5G18830; SPL8, AT1G02065; SPL9, AT2G42200; SPL10, AT1G27370; SPL11, AT1G27360; SPL12, AT3G60030; SPL13A, AT5G50570; SPL13B, AT5G50670; SPL14, AT1G20980; SPL15, AT3G57920.

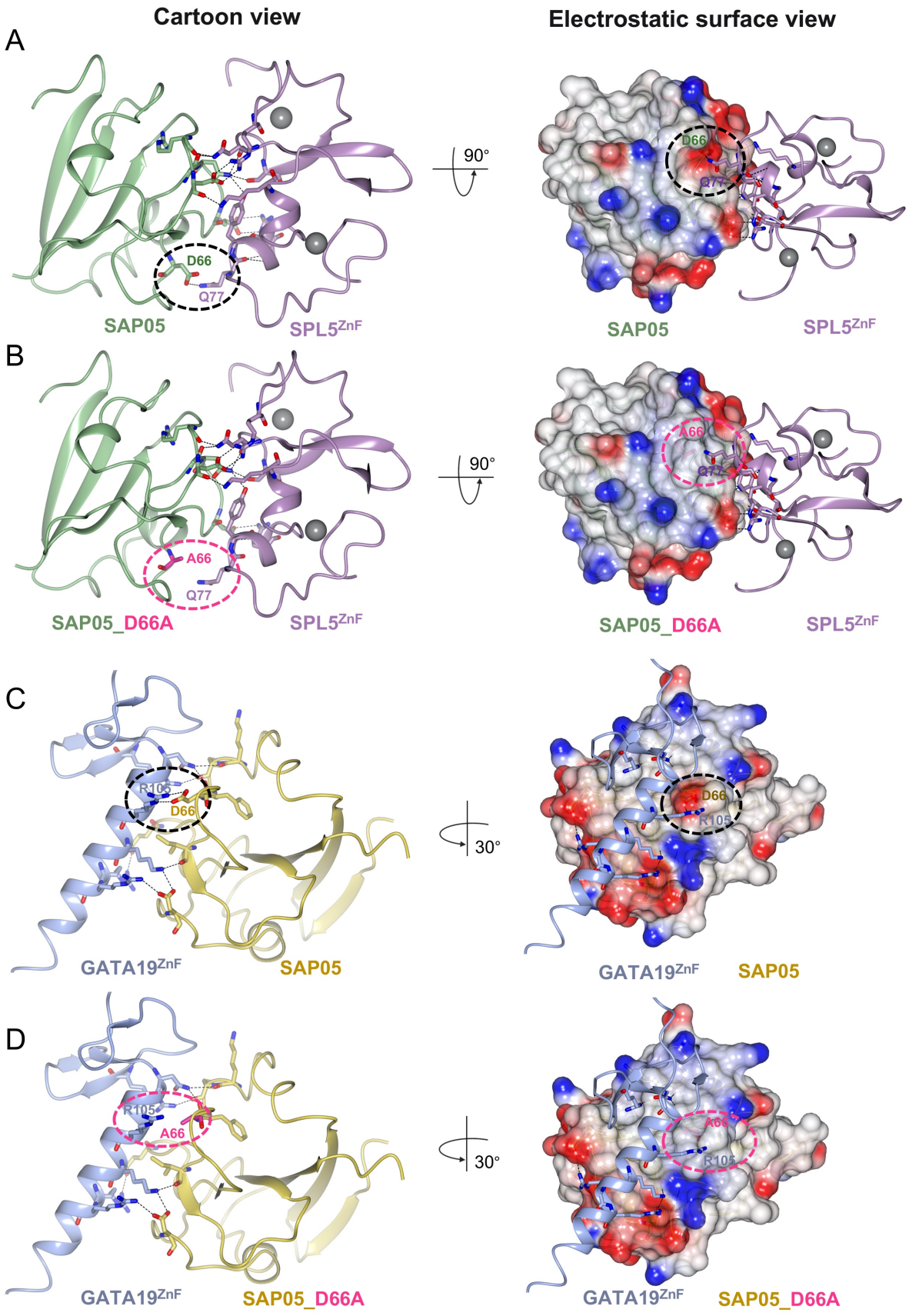
Cartoon view
Electrostatic surface view
A
D66
Q77
90°
SAP05
SPL5ZnF
B
A66
Q77
SAP05_D66A
C
R105
30°
GATA19ZnF
D

Fig. S13. SAP05 D66 creates an electronegative surface at the binding interface with zinc-fingers of SPL and GATA. (A) SAP05 D66 interacts with Q77 on SPL5^{ZnF} (left) and present negative surface on the binding interface (right). (B) SAP05 D66A lost the interaction with SPL5 Q77 (left), and the electronegativity on the interaction surface is reduced (right). (C) SAP05 D66 interacts with GATA19^{ZnF} R105 based on AlphaFold predicted top-rank structure (left) and present negative surface at the interface (right). (D) SAP05 D66A lost the interaction with GATA19 R105 (left), and the electronegativity on the interaction surface is reduced (right).

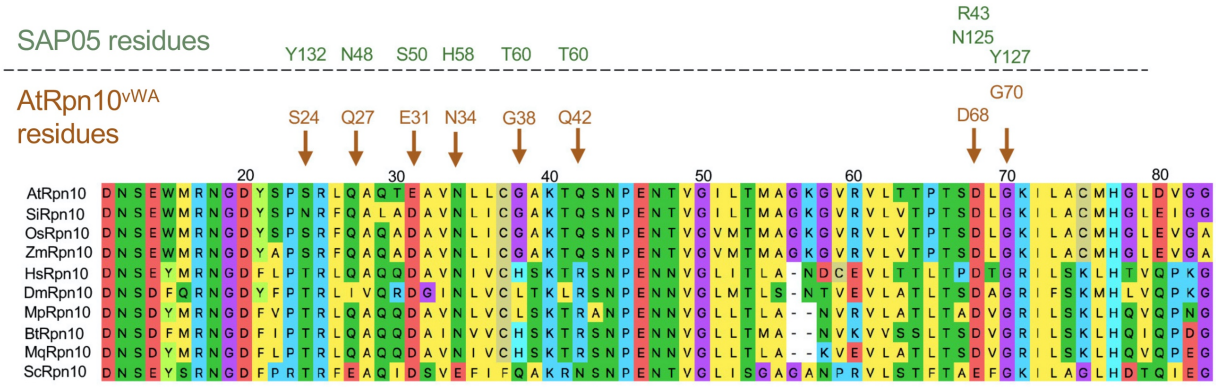

Fig. S14. Multiple sequence alignment of Rpn10^{vWA} from different species. The conserved Rpn10^{vWA} residues involved in interaction with SAP05 are indicated with orange arrows, and the corresponding SAP05 residues are shown on top in green. Sequence alignment was conducted with MUSCLE in MEGA11 software. AtRpn10, *Arabidopsis thaliana* Rpn10 (Uniprot ID: P55034); SlRpn10, *Solanum lycopersicum* Rpn10 (Uniprot ID: A0A3Q7F6N7); OsRpn10, *Oryza sativa* Rpn10 (Uniprot ID: O82143); ZmRpn10, *Zea mays* Rpn10 (Uniprot ID: B6TK61); HsRpn10, *Homo sapiens* Rpn10 (Uniprot ID: Q5VWC4); DmRpn10, *Drosophila melanogaster* Rpn10 (Uniprot ID: P55035); MpRpn10, *Myzus persicae* Rpn 10 (GenBank: XP_022181722.1); BtRpn10, *Bemisia tabaci* Rpn10 (GenBank: XP_018915695); MqRpn10, *Macrosteles quadrilineatus* Rpn10; ScRpn10, *Saccharomyces cerevisiae* Rpn10 (Uniprot ID: P38886).

Fig. S15. Sequence alignment of Rpn10 vWA domains from *Spinacia oleracea* and *A. thaliana.* The conserved vWA residues involved in interaction with SAP05 are marked with grey background. Residues interacting with 26S proteasome are marked pink with pink arrows. SoRpn10^{vWA} sequence was extracted from the structure of spinach 19S proteasome (PDB 8AMZ). Sequence alignment was conducted with MUSCLE in MEGA11 software and residues interacting with 26S proteasome were analyzed with CCP4mg.

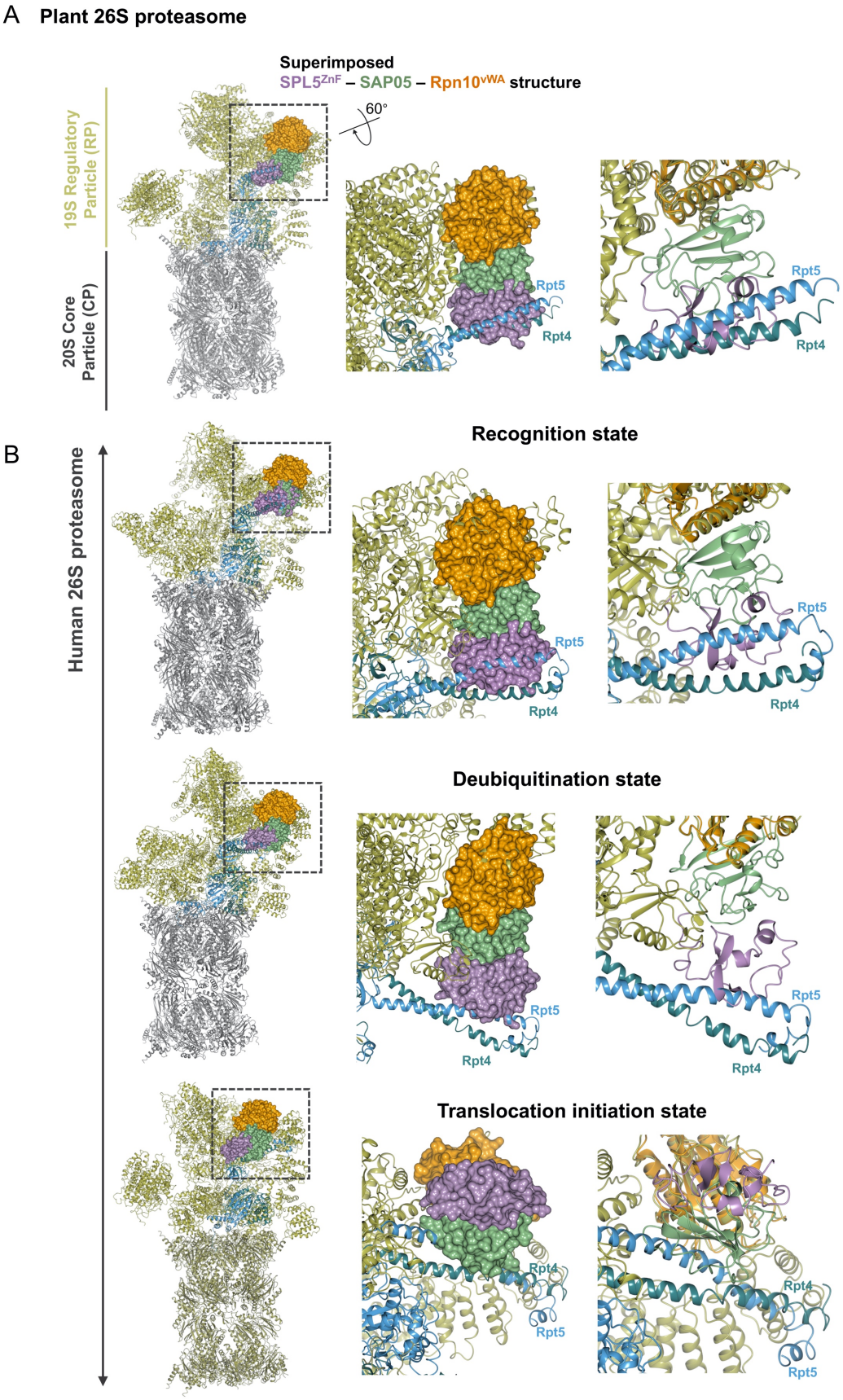
A
Plant 26S proteasome
Superimposed
SPL5ZnF – SAP05 – Rpn10vWA structure
60°
19S Regulatory Particle (RP)
20S Core Particle (CP)
Rpt5
Rpt4
B
Human 26S proteasome
Recognition state
Deubiquitination state
Translocation initiation state

Fig. S16. Modelling of the Rpn10^{vWA} – SAP05 – SPL5^{ZnF} ternary structure with plant and human 26S proteasome components show potential clashes. (A) Structural superimposition of the ternary structure on the spinach 26S proteasome (PDB 7QVE and PDB 8AMZ). Left, overview of the superimposition. Middle, enlarged surface view of the superimposed part within the dashed box. Right, enlarged cartoon view of the superimposed part. (B) Structural superimposition of the ternary structure on substrate recognition state (PDB 6MSD), deubiquitination state (PDB 6MSE) translocation initiation state (PDB 6MSH) of human 26S proteasome. Left, overview of the superimposition. Middle, enlarged surface view of the superimposed part within the dashed box. Right, enlarged cartoon view of the superimposed part. The superimposed structures highlight the clashes between SPL5^{ZnF} and two α-helices of 19S RP subunits, which are homologs of *A. thaliana* Rpt4 (turquoise) and Rpt5 (blue).

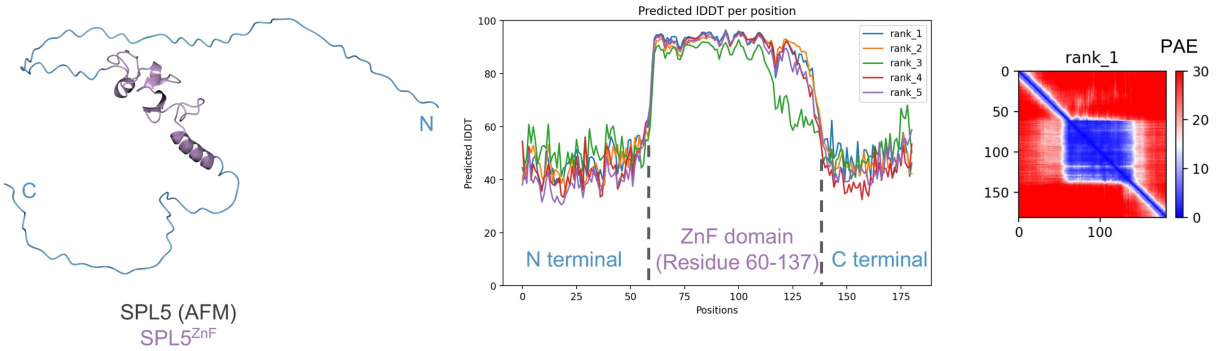

Fig. S17. Structural prediction of full-length SPL5. Left, AlphaFold model (AFM) for full-length SPL5 protein. N- and C- terminal parts are colored blue. $SPL5^{ZnF}$ domain is shown in purple. Middle, the predicted local Distance Difference Test (lDDT) value of SPL5 model, showing the quality of predicted models. Best model (rank_1) was shown in left panel. N- and C- terminal, and ZnF domain are labelled inside, with the same color as left. Right, predicted aligned error (PAE) of the rank_1 model. Blue means lower error scores, red means higher error scores.

Table S1. Analysis of residues on SAP05 – SPL5^{ZnF} interface from PDBsum

PDB code: 8pfc												
Hydrogen bonds												
	Atom no.	Atom name	Res name	Res no.	Chain		Atom no.	Atom name	Res name	Res no.	Chain	Distance
1	262	OD1	ASP	66	A	<-->	931	NE2	GLN	77	B	3.10
2	350	ND2	ASN	77	A	<-->	943	OH	TYR	78	B	3.16
3	350	ND2	ASN	77	A	<-->	1154	O	GLN	105	B	2.84
4	371	OE1	GLU	80	A	<-->	987	NE2	HIS	82	B	3.11
5	559	O	ARG	104	A	<-->	1159	NE2	GLN	105	B	2.64
6	578	O	ASP	106	A	<-->	1051	NZ	LYS	90	B	3.23
7	581	OD1	ASP	106	A	<-->	1051	NZ	LYS	90	B	3.11
8	581	OD1	ASP	106	A	<-->	1297	NH1	ARG	121	B	3.06
9	582	OD2	ASP	106	A	<-->	1298	NH2	ARG	121	B	2.97
Non-bonded contacts												
	Atom no.	Atom name	Res name	Res no.	Chain		Atom no.	Atom name	Res name	Res no.	Chain	Distance
1	261	CG	ASP	66	A	<-->	931	NE2	GLN	77	B	3.77
2	262	OD1	ASP	66	A	<-->	931	NE2	GLN	77	B	3.10
3	263	OD2	ASP	66	A	<-->	923	N	GLN	77	B	3.85
4	281	CG2	THR	68	A	<-->	931	NE2	GLN	77	B	3.81
5	289	CD2	LEU	69	A	<-->	921	CE	LYS	76	B	3.76
6	317	NH1	ARG	73	A	<-->	921	CE	LYS	76	B	3.54
7	342	O	GLY	76	A	<-->	1159	NE2	GLN	105	B	3.58
8	347	CB	ASN	77	A	<-->	1154	O	GLN	105	B	3.32
9	348	CG	ASN	77	A	<-->	1154	O	GLN	105	B	3.55
10	350	ND2	ASN	77	A	<-->	943	OH	TYR	78	B	3.16
11	350	ND2	ASN	77	A	<-->	1154	O	GLN	105	B	2.84
12	350	ND2	ASN	77	A	<-->	1180	OG	SER	108	B	3.20
13	363	CB	ALA	79	A	<-->	940	CE1	TYR	78	B	3.80
14	363	CB	ALA	79	A	<-->	987	NE2	HIS	82	B	3.89
15	363	CB	ALA	79	A	<-->	1180	OG	SER	108	B	3.67
16	367	O	GLU	80	A	<-->	938	CD1	TYR	78	B	3.41
17	367	O	GLU	80	A	<-->	986	CE1	HIS	82	B	3.71
18	369	CG	GLU	80	A	<-->	976	NH1	ARG	81	B	3.42
19	370	CD	GLU	80	A	<-->	976	NH1	ARG	81	B	3.52
20	371	OE1	GLU	80	A	<-->	986	CE1	HIS	82	B	3.42
21	371	OE1	GLU	80	A	<-->	987	NE2	HIS	82	B	3.11
22	372	OE2	GLU	80	A	<-->	976	NH1	ARG	81	B	3.53
23	376	O	PHE	81	A	<-->	936	CB	TYR	78	B	3.51
24	377	CB	PHE	81	A	<-->	932	N	TYR	78	B	3.73
25	378	CG	PHE	81	A	<-->	927	CB	GLN	77	B	3.66
26	380	CD2	PHE	81	A	<-->	927	CB	GLN	77	B	3.65
27	381	CE1	PHE	81	A	<-->	929	CD	GLN	77	B	3.82
28	381	CE1	PHE	81	A	<-->	930	OE1	GLN	77	B	3.39
29	382	CE2	PHE	81	A	<-->	977	NH2	ARG	81	B	3.82
30	383	CZ	PHE	81	A	<-->	930	OE1	GLN	77	B	3.40
31	401	CB	ILE	84	A	<-->	920	CD	LYS	76	B	3.87
32	404	CD1	ILE	84	A	<-->	955	OH	TYR	79	B	3.81

33	416	CZ2	TRP	85	A	<-->	955	OH	TYR	79	B	3.45
34	417	CZ3	TRP	85	A	<-->	1020	OE2	GLU	86	B	3.81
35	418	CH2	TRP	85	A	<-->	955	OH	TYR	79	B	3.35
36	418	CH2	TRP	85	A	<-->	1020	OE2	GLU	86	B	3.90
37	553	CB	THR	103	A	<-->	1157	CD	GLN	105	B	3.83
38	553	CB	THR	103	A	<-->	1158	OE1	GLN	105	B	3.84
39	554	OG1	THR	103	A	<-->	1304	OG	SER	122	B	3.89
40	555	CG2	THR	103	A	<-->	1160	N	GLN	106	B	3.78
41	555	CG2	THR	103	A	<-->	1161	CA	GLN	106	B	3.54
42	555	CG2	THR	103	A	<-->	1164	CB	GLN	106	B	3.50
43	556	N	ARG	104	A	<-->	1159	NE2	GLN	105	B	3.84
44	558	C	ARG	104	A	<-->	1159	NE2	GLN	105	B	3.67
45	559	O	ARG	104	A	<-->	1157	CD	GLN	105	B	3.76
46	559	O	ARG	104	A	<-->	1159	NE2	GLN	105	B	2.64
47	578	O	ASP	106	A	<-->	1050	CE	LYS	90	B	3.09
48	578	O	ASP	106	A	<-->	1051	NZ	LYS	90	B	3.23
49	580	CG	ASP	106	A	<-->	1050	CE	LYS	90	B	3.63
50	580	CG	ASP	106	A	<-->	1051	NZ	LYS	90	B	3.77
51	580	CG	ASP	106	A	<-->	1159	NE2	GLN	105	B	3.71
52	580	CG	ASP	106	A	<-->	1297	NH1	ARG	121	B	3.80
53	580	CG	ASP	106	A	<-->	1298	NH2	ARG	121	B	3.66
54	581	OD1	ASP	106	A	<-->	1050	CE	LYS	90	B	3.45
55	581	OD1	ASP	106	A	<-->	1051	NZ	LYS	90	B	3.11
56	581	OD1	ASP	106	A	<-->	1296	CZ	ARG	121	B	3.82
57	581	OD1	ASP	106	A	<-->	1297	NH1	ARG	121	B	3.06
58	581	OD1	ASP	106	A	<-->	1298	NH2	ARG	121	B	3.66
59	582	OD2	ASP	106	A	<-->	1050	CE	LYS	90	B	3.61
60	582	OD2	ASP	106	A	<-->	1159	NE2	GLN	105	B	3.77
61	582	OD2	ASP	106	A	<-->	1296	CZ	ARG	121	B	3.86
62	582	OD2	ASP	106	A	<-->	1297	NH1	ARG	121	B	3.84
63	582	OD2	ASP	106	A	<-->	1298	NH2	ARG	121	B	2.97

Salt bridges

	Atom no.	Atom name	Res name	Res no.	Chain		Atom no.	Atom name	Res name	Res no.	Chain	Distance
1	372	OE2	GLU	80	A	<-->	976	NH1	ARG	81	B	3.53
2	371	OE1	GLU	80	A	<-->	987	NE2	HIS	82	B	3.11
3	581	OD1	ASP	106	A	<-->	1051	NZ	LYS	90	B	3.11
4	582	OD2	ASP	106	A	<-->	1298	NH2	ARG	121	B	2.97

Table S2. Analysis of residues on SAP05 – Rpn10^{vWA} interface from PDBsum

PDB code: 8pfd												
Hydrogen bonds												
	Atom no.	Atom name	Res name	Res no.	Chain		Atom no.	Atom name	Res name	Res no.	Chain	Distance
1	62	NH1	ARG	43	A	<-->	1289	OD2	ASP	68	B	3.10
2	110	N	SER	50	A	<-->	1031	OE2	GLU	31	B	2.57
3	115	OG	SER	50	A	<-->	1031	OE2	GLU	31	B	2.48
4	181	NE2	HIS	58	A	<-->	1047	O	ASN	34	B	3.08
5	181	NE2	HIS	58	A	<-->	1050	OD1	ASN	34	B	2.86
6	731	ND2	ASN	125	A	<-->	1288	OD1	ASP	68	B	3.23
Non-bonded contacts												
	Atom no.	Atom name	Res name	Res no.	Chain		Atom no.	Atom name	Res name	Res no.	Chain	Distance
1	59	CD	ARG	43	A	<-->	1300	C	GLY	70	B	3.80
2	59	CD	ARG	43	A	<-->	1301	O	GLY	70	B	3.68
3	59	CD	ARG	43	A	<-->	1331	CB	ALA	74	B	3.75
4	61	CZ	ARG	43	A	<-->	1303	CA	LYS	71	B	3.84
5	62	NH1	ARG	43	A	<-->	1289	OD2	ASP	68	B	3.10
6	62	NH1	ARG	43	A	<-->	1302	N	LYS	71	B	3.78
7	63	NH2	ARG	43	A	<-->	1307	CG	LYS	71	B	3.89
8	77	CG1	VAL	45	A	<-->	1301	O	GLY	70	B	3.67
9	77	CG1	VAL	45	A	<-->	1327	N	ALA	74	B	3.78
10	78	CG2	VAL	45	A	<-->	1301	O	GLY	70	B	3.85
11	82	O	ASN	46	A	<-->	1350	CB	HIS	77	B	3.87
12	82	O	ASN	46	A	<-->	1353	CD2	HIS	77	B	3.58
13	83	CB	ASN	46	A	<-->	1351	CG	HIS	77	B	3.89
14	83	CB	ASN	46	A	<-->	1353	CD2	HIS	77	B	3.36
15	83	CB	ASN	46	A	<-->	1355	NE2	HIS	77	B	3.48
16	92	CG1	VAL	47	A	<-->	1051	ND2	ASN	34	B	3.25
17	97	O	ASN	48	A	<-->	1001	NE2	GLN	27	B	3.54
18	101	ND2	ASN	48	A	<-->	1353	CD2	HIS	77	B	3.89
19	103	CA	LEU	49	A	<-->	1031	OE2	GLU	31	B	3.55
20	104	C	LEU	49	A	<-->	1031	OE2	GLU	31	B	3.49
21	110	N	SER	50	A	<-->	1001	NE2	GLN	27	B	3.78
22	110	N	SER	50	A	<-->	1029	CD	GLU	31	B	3.69
23	110	N	SER	50	A	<-->	1031	OE2	GLU	31	B	2.57
24	111	CA	SER	50	A	<-->	1031	OE2	GLU	31	B	3.39
25	114	CB	SER	50	A	<-->	1029	CD	GLU	31	B	3.86
26	114	CB	SER	50	A	<-->	1030	OE1	GLU	31	B	3.81
27	114	CB	SER	50	A	<-->	1031	OE2	GLU	31	B	3.13
28	115	OG	SER	50	A	<-->	1029	CD	GLU	31	B	3.20
29	115	OG	SER	50	A	<-->	1030	OE1	GLU	31	B	3.21
30	115	OG	SER	50	A	<-->	1031	OE2	GLU	31	B	2.48
31	143	O	ILE	54	A	<-->	1059	CD2	LEU	35	B	3.55
32	145	CG1	ILE	54	A	<-->	1031	OE2	GLU	31	B	3.78
33	165	C	LYS	57	A	<-->	1059	CD2	LEU	35	B	3.65
34	166	O	LYS	57	A	<-->	1059	CD2	LEU	35	B	3.70
35	172	N	HIS	58	A	<-->	1059	CD2	LEU	35	B	3.50
36	173	CA	HIS	58	A	<-->	1059	CD2	LEU	35	B	3.39
37	176	CB	HIS	58	A	<-->	1059	CD2	LEU	35	B	3.55

38	177	CG	HIS	58	A	<-->	1059	CD2	LEU	35	B	3.85
39	179	CD2	HIS	58	A	<-->	1047	O	ASN	34	B	3.72
40	179	CD2	HIS	58	A	<-->	1050	OD1	ASN	34	B	3.37
41	179	CD2	HIS	58	A	<-->	1059	CD2	LEU	35	B	3.75
42	180	CE1	HIS	58	A	<-->	1075	CA	GLY	38	B	3.46
43	181	NE2	HIS	58	A	<-->	1046	C	ASN	34	B	3.81
44	181	NE2	HIS	58	A	<-->	1047	O	ASN	34	B	3.08
45	181	NE2	HIS	58	A	<-->	1049	CG	ASN	34	B	3.85
46	181	NE2	HIS	58	A	<-->	1050	OD1	ASN	34	B	2.86
47	184	C	GLU	59	A	<-->	1104	CG	GLN	42	B	3.83
48	185	O	GLU	59	A	<-->	1104	CG	GLN	42	B	3.40
49	185	O	GLU	59	A	<-->	1105	CD	GLN	42	B	3.69
50	192	CA	THR	60	A	<-->	1106	OE1	GLN	42	B	3.88
51	196	OG1	THR	60	A	<-->	1075	CA	GLY	38	B	3.55
52	196	OG1	THR	60	A	<-->	1077	O	GLY	38	B	3.76
53	196	OG1	THR	60	A	<-->	1106	OE1	GLN	42	B	3.67
54	196	OG1	THR	60	A	<-->	1297	CD2	LEU	69	B	3.53
55	224	CD	LYS	63	A	<-->	1107	NE2	GLN	42	B	3.74
56	729	CG	ASN	125	A	<-->	1299	CA	GLY	70	B	3.80
57	730	OD1	ASN	125	A	<-->	1299	CA	GLY	70	B	3.38
58	731	ND2	ASN	125	A	<-->	1288	OD1	ASP	68	B	3.23
59	751	OH	TYR	127	A	<-->	1292	C	LEU	69	B	3.82
60	751	OH	TYR	127	A	<-->	1294	CB	LEU	69	B	3.59
61	751	OH	TYR	127	A	<-->	1298	N	GLY	70	B	3.26
62	751	OH	TYR	127	A	<-->	1299	CA	GLY	70	B	3.61
63	800	CD1	TYR	132	A	<-->	998	CG	GLN	27	B	3.71
64	800	CD1	TYR	132	A	<-->	999	CD	GLN	27	B	3.56
65	800	CD1	TYR	132	A	<-->	1000	OE1	GLN	27	B	3.74
66	802	CE1	TYR	132	A	<-->	997	CB	GLN	27	B	3.69
67	802	CE1	TYR	132	A	<-->	998	CG	GLN	27	B	3.60
68	802	CE1	TYR	132	A	<-->	999	CD	GLN	27	B	3.82
69	802	CE1	TYR	132	A	<-->	1000	OE1	GLN	27	B	3.87
70	804	CZ	TYR	132	A	<-->	997	CB	GLN	27	B	3.81
71	804	CZ	TYR	132	A	<-->	998	CG	GLN	27	B	3.85
72	805	OH	TYR	132	A	<-->	968	N	SER	24	B	3.58
73	805	OH	TYR	132	A	<-->	972	CB	SER	24	B	3.15

Salt bridges

	Atom no.	Atom name	Res name	Res no.	Chain		Atom no.	Atom name	Res name	Res no.	Chain	Distance
1	62	NH1	ARG	43	A	<-->	1289	OD2	ASP	68	B	3.1

References

1. N. S. Berrow *et al.*, A versatile ligation-independent cloning method suitable for high-throughput expression screening applications. *Nucleic Acids Res.* **35**, e45 (2007).
2. R. M. Benoit, R. N. Wilhelm, D. Scherer-Becker, C. Ostermeier, An improved method for fast, robust, and seamless integration of DNA fragments into multiple plasmids. *Protein Expr. Purif.* **45**, 66-71 (2006).
3. L. E. Bird *et al.*, Application of In-Fusion™ cloning for the parallel construction of E. coli expression vectors. *Methods Mol. Biol.* **1116**, 209-234 (2014).
4. H. Wickham, ggplot2. *Wiley Interdisciplinary Reviews: Computational Statistics* **3**, 180-185 (2011).
5. G. Winter *et al.*, DIALS: implementation and evaluation of a new integration package. *Acta Crystallogr. D Struct. Biol.* **74**, 85-97 (2018).
6. G. Winter, XIA2: an expert system for macromolecular crystallography data reduction. *J. Appl. Cryst.* **43**, 186-190 (2010).
7. P. R. Evans, G. N. Murshudov, How good are my data and what is the resolution? *Acta Crystallogr. D Biol. Crystallogr.* **69**, 1204-1214 (2013).
8. M. D. Winn *et al.*, Overview of the CCP4 suite and current developments. *Acta Crystallogr. D Biol. Crystallogr.* **67**, 235-242 (2011).
9. P. Skubák *et al.*, A new MR-SAD algorithm for the automatic building of protein models from low-resolution X-ray data and a poor starting model. *IUCrJ* **5**, 166-171 (2018).
10. P. Emsley, B. Lohkamp, W. G. Scott, K. Cowtan, Features and development of Coot. *Acta Crystallogr. D Biol. Crystallogr.* **66**, 486-501 (2010).
11. G. N. Murshudov *et al.*, REFMAC5 for the refinement of macromolecular crystal structures. *Acta Crystallogr. D Biol. Crystallogr.* **67**, 355-367 (2011).
12. A. J. McCoy *et al.*, Phaser crystallographic software. *J. Appl. Crystallogr.* **40**, 658-674 (2007).
13. A. Waterhouse *et al.*, SWISS-MODEL: homology modelling of protein structures and complexes. *Nucleic Acids Res.* **46**, W296-w303 (2018).

14. Y. Zhu *et al.*, Structural mechanism for nucleotide-driven remodeling of the AAA-ATPase unfoldase in the activated human 26S proteasome. *Nat. Commun.* **9**, 1360 (2018).
15. S. McNicholas, E. Potterton, K. S. Wilson, M. E. Noble, Presenting your structures: the CCP4mg molecular-graphics software. *Acta Crystallogr. D Biol. Crystallogr.* **67**, 386-394 (2011).
16. J. L. Hartley, G. F. Temple, M. A. Brasch, DNA cloning using in vitro site-specific recombination. *Genome Res.* **10**, 1788-1795 (2000).
17. X. Liang, L. Peng, C. H. Baek, F. Katzen, Single step BP/LR combined Gateway reactions. *Biotechniques* **55**, 265-268 (2013).
18. W. Huang *et al.*, Parasitic modulation of host development by ubiquitin-independent protein degradation. *Cell* **184**, 5201-5214.e12 (2021).
19. S. D. Yoo, Y. H. Cho, J. Sheen, Arabidopsis mesophyll protoplasts: a versatile cell system for transient gene expression analysis. *Nat. Protoc.* **2**, 1565-1572 (2007).

Uncropped Gels and Western Blots

Fig. 1F

Coomassie stained gels showing the proteins from different gel filtration fractions. Red dashed rectangles indicate the cropped image shown in the main and supplementary figures.

GF of SPL5^{ZnF}-SAP05-Rpn10^{vWA} ternary complex

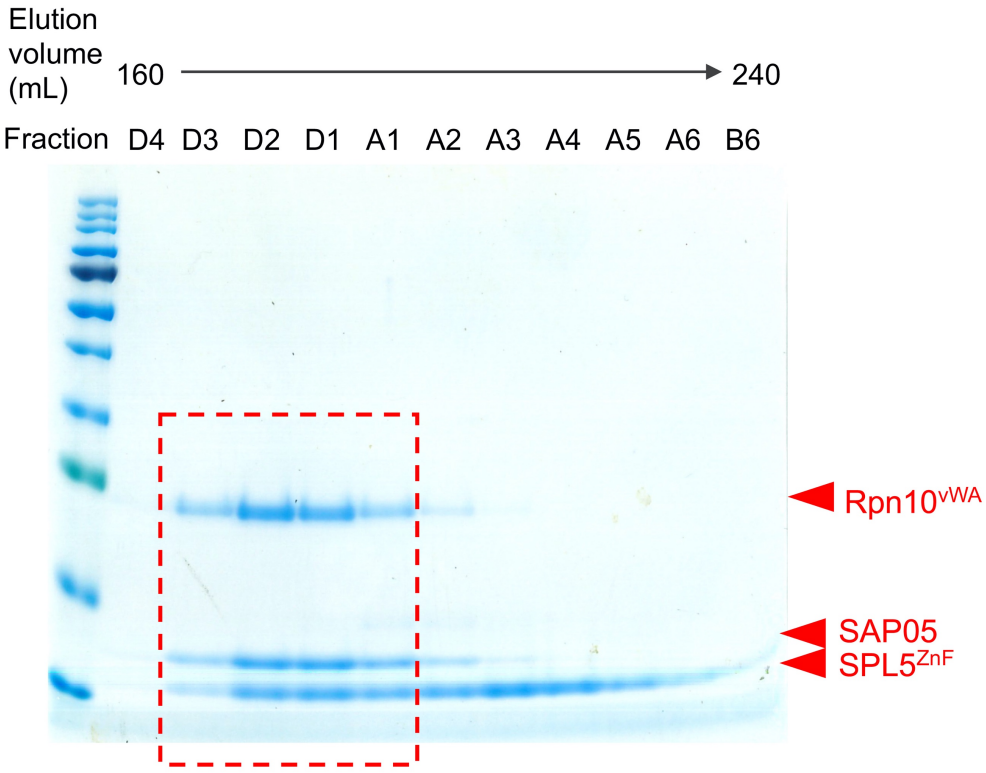

SI Appendix Fig. S1B

GF of SAP05-Rpn10^{vWA} complex

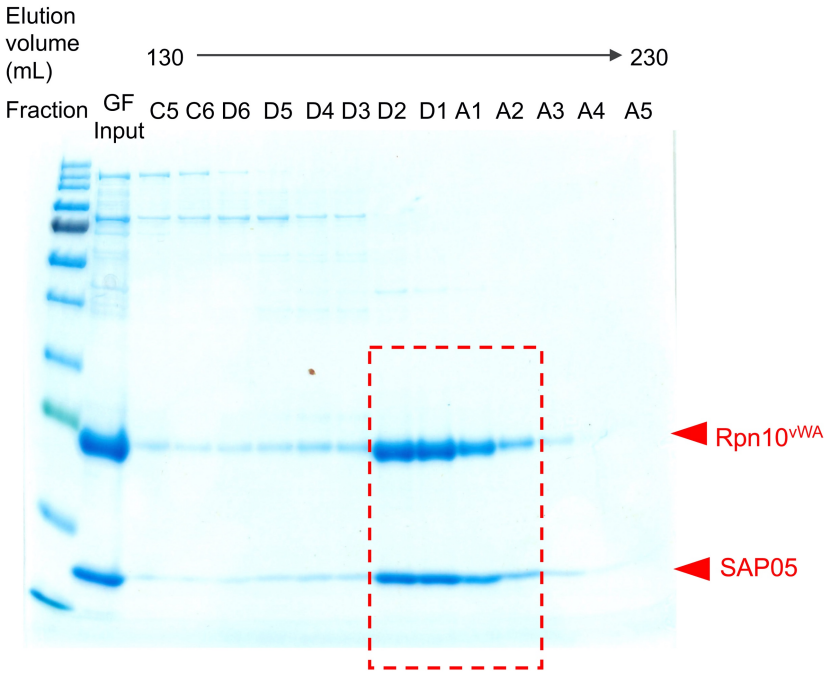

GF of SAP05-SPL5^{ZnF} complex

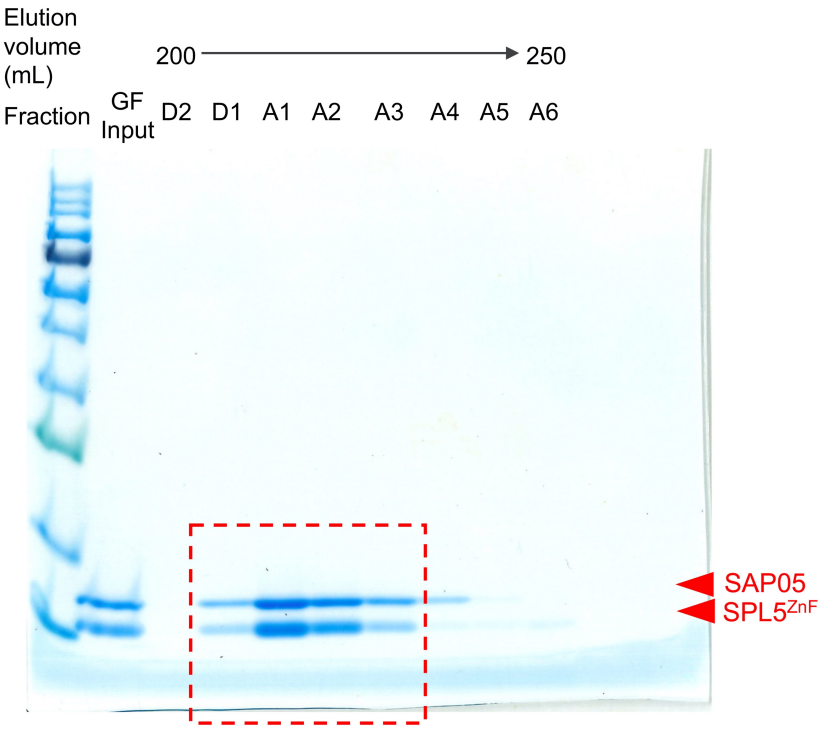

GF of SAP05

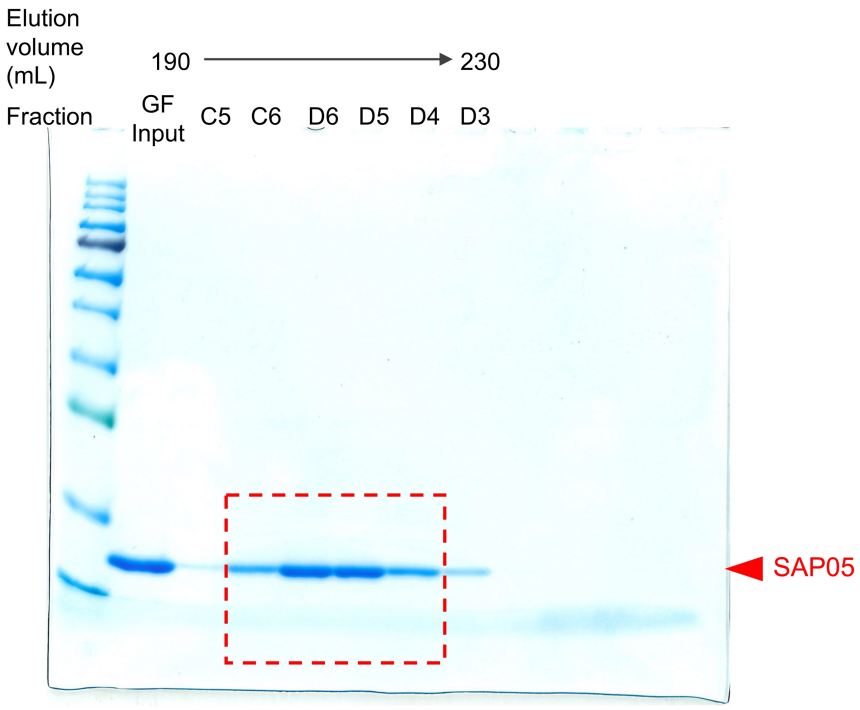

GF of SPL5^{ZnF}

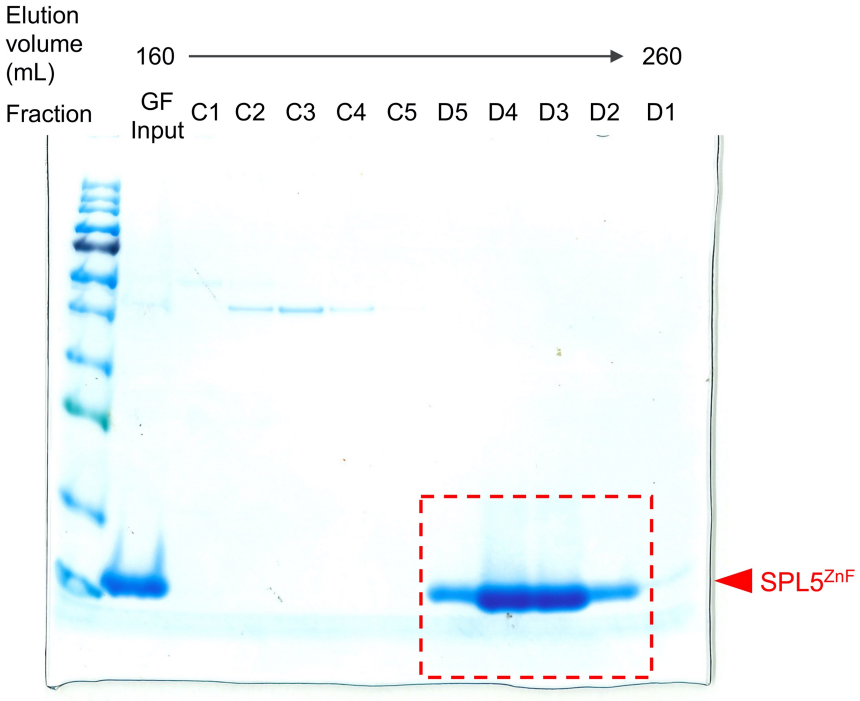

Fig. 2D

The degradation efficiency (Rel HA/rbcL) was calculated as the HA intensity divided by the RuBisCo large subunit (rbcL) intensity from the same sample, normalized to the intensity of the sample with the highest ratio from the same leaf. The expected size for SAP05, SPL5, and GATA19 is indicated. Experiments included in the main figures are indicated with red dashed rectangles. *Failed experiments due to errors in controls.

	SAP05 D66A											
Leaf	Repeat 1*				Repeat 2				Repeat 3			
HA-SPL5	+	+	+	-	+	+	+	-	+	+	+	-
SAP05 (WT)	+	-	-	-	+	-	-	-	+	-	-	-
SAP05 (mut)	-	+	-	+	-	+	-	+	-	+	-	+
Lane	A	B	C	D	E	F	G	H	I	J	K	L
Rel HA/rbcL	0.24	1.00	0.03	0.00	0.10	0.88	1.00	0.00	0.12	0.74	1.00	0.00

	SAP05 D66E											
Leaf	Repeat 1				Repeat 2*				Repeat 3			
HA-SPL5	+	+	+	-	+	+	+	-	+	+	+	-
SAP05 (WT)	+	-	-	-	+	-	-	-	+	-	-	-
SAP05 (mut)	-	+	-	+	-	+	-	+	-	+	-	+
Lane	1	2	3	4	5	6	7	8	9	10	11	12
Rel HA/rbcL	0.08	0.09	1.00	0.00	0.88	1.00	0.37	0.00	0.20	0.19	1.00	0.00

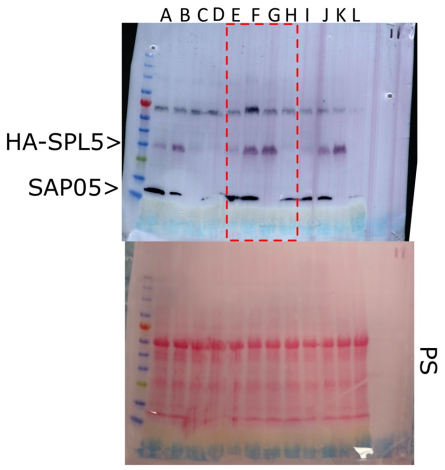

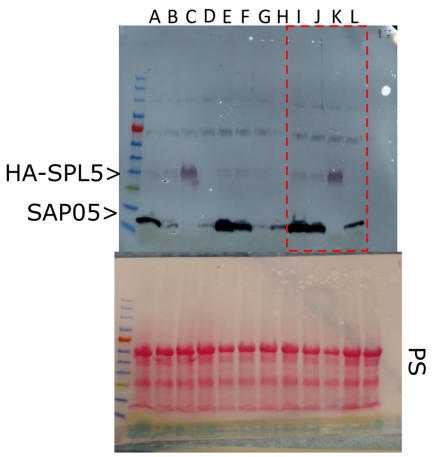

	SAP05 G76W											
Leaf	Repeat 1				Repeat 2				Repeat 3			
HA-SPL5	+	+	+	-	+	+	+	-	+	+	+	-
SAP05 (WT)	+	-	-	-	+	-	-	-	+	-	-	-
SAP05 (mut)	-	+	-	+	-	+	-	+	-	+	-	+
Lane	A	B	C	D	E	F	G	H	I	J	K	L
Rel HA/rbcL	0.04	0.63	1.00	0.01	0.10	0.60	1.00	0.00	0.09	0.77	1.00	0.00

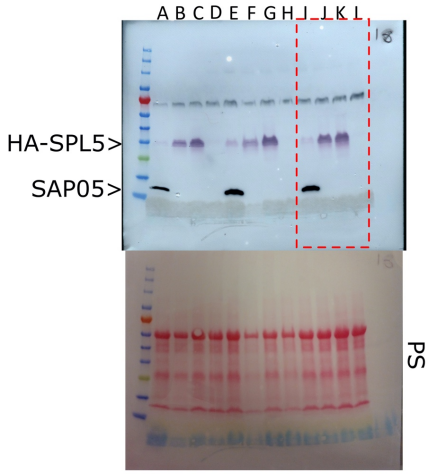

	SAP05 N77D											
Leaf	Repeat 1				Repeat 2				Repeat 3			
HA-SPL5	+	+	+	-	+	+	+	-	+	+	+	-
SAP05 (WT)	+	-	-	-	+	-	-	-	+	-	-	-
SAP05 (mut)	-	+	-	+	-	+	-	+	-	+	-	+
Lane	A	B	C	D	E	F	G	H	I	J	K	L
Rel HA/rbcL	0.11	0.21	1.00	0.01	0.19	0.64	1.00	0.01	0.15	0.57	1.00	0.03

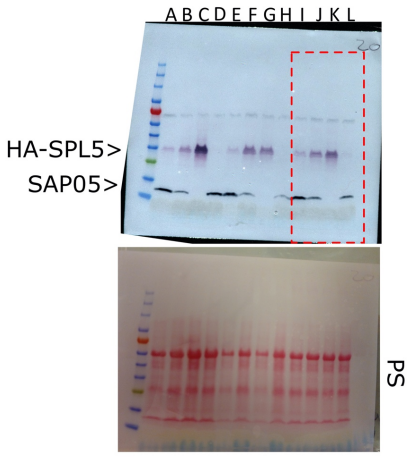

	SAP05 N77A											
Leaf	Repeat 1				Repeat 2*				Repeat 3			
HA-SPL5	+	+	+	-	+	+	+	-	+	+	+	-
SAP05 (WT)	+	-	-	-	+	-	-	-	+	-	-	-
SAP05 (mut)	-	+	-	+	-	+	-	+	-	+	-	+
Lane	A	B	C	D	E	F	G	H	I	J	K	L
Rel HA/rbcL	0.06	0.09	1.00	0.02	1.00	0.82	0.62	0.00	0.19	0.08	1.00	0.00

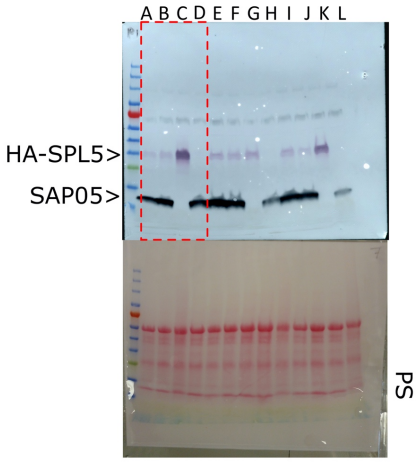

	SAP05 N77R											
Leaf	Repeat 1				Repeat 2				Repeat 3			
HA-SPL5	+	+	+	-	+	+	+	-	+	+	+	-
SAP05 (WT)	+	-	-	-	+	-	-	-	+	-	-	-
SAP05 (mut)	-	+	-	+	-	+	-	+	-	+	-	+
Lane	A	B	C	D	E	F	G	H	I	J	K	L
Rel HA/rbcL	0.19	1.00	0.59	0.02	0.14	1.00	0.70	0.00	0.10	1.00	0.87	0.01

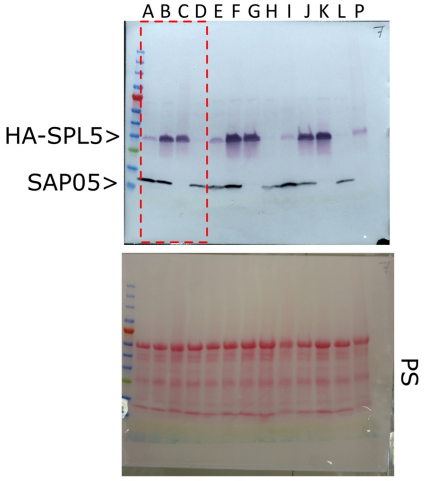

	SAP05 E80A											
Leaf	Repeat 1				Repeat 2				Repeat 3			
HA-SPL5	+	+	+	-	+	+	+	-	+	+	+	-
SAP05 (WT)	+	-	-	-	+	-	-	-	+	-	-	-
SAP05 (mut)	-	+	-	+	-	+	-	+	-	+	-	+
Lane	A	B	C	D	E	F	G	H	I	J	K	L
Rel HA/rbcL	0.12	0.18	1.00	0.01	0.08	0.06	1.00	0.02	0.30	0.18	1.00	0.02

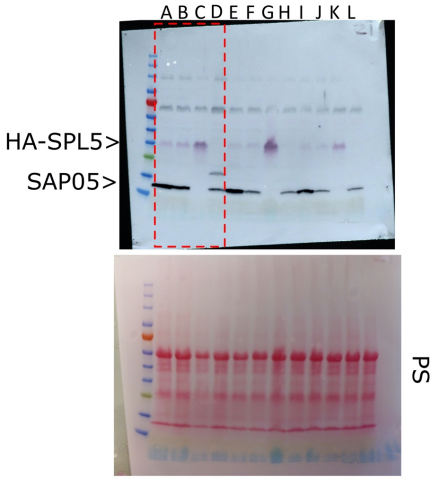

	SAP05 E80R											
Leaf	Repeat 1				Repeat 2				Repeat 3			
HA-SPL5	+	+	+	-	+	+	+	-	+	+	+	-
SAP05 (WT)	+	-	-	-	+	-	-	-	+	-	-	-
SAP05 (mut)	-	+	-	+	-	+	-	+	-	+	-	+
Lane	A	B	C	D	E	F	G	H	I	J	K	L
Rel HA/rbcL	0.08	0.09	1.00	0.00	0.22	0.17	1.00	0.11	0.12	0.12	1.00	0.01

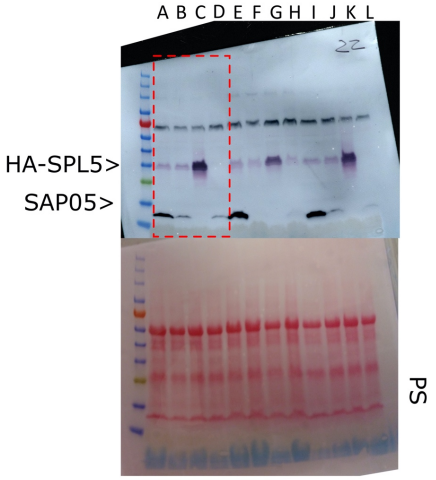

	SAP05 D106A											
Leaf	Repeat 1				Repeat 2*				Repeat 3			
HA-SPL5	+	+	+	-	+	+	+	-	+	+	+	-
SAP05 (WT)	+	-	-	-	+	-	-	-	+	-	-	-
SAP05 (mut)	-	+	-	+	-	+	-	+	-	+	-	+
Lane	A	B	C	D	E	F	G	H	I	J	K	L
Rel HA/rbcL	0.10	1.00	0.85	0.00	0.43	1.00	0.61	0.04	0.11	1.00	01.02	0.01

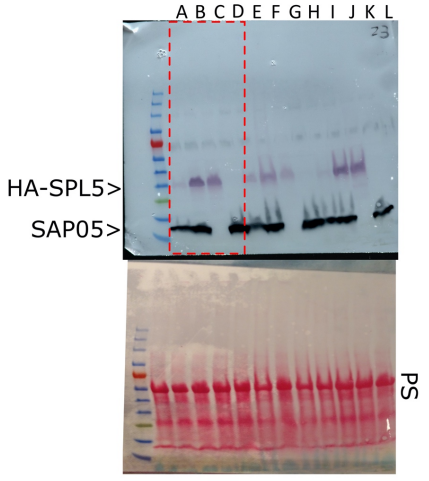

	SAP05 D106R											
Leaf	Repeat 1				Repeat 2*				Repeat 3			
HA-SPL5	+	+	+	-	+	+	+	-	+	+	+	-
SAP05 (WT)	+	-	-	-	+	-	-	-	+	-	-	-
SAP05 (mut)	-	+	-	+	-	+	-	+	-	+	-	+
Lane	A	B	C	D	E	F	G	H	I	J	K	L
Rel HA/rbcL	0.03	1.00	0.51	0.01	0.10	1.00	0.07	0.05	0.04	1.00	0.61	0.07

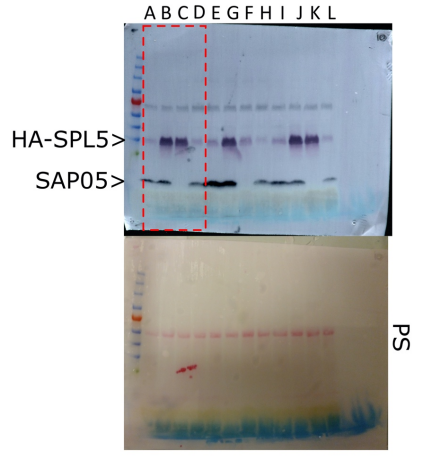

Fig. 2F

	SAP05 D66A											
Leaf	Repeat 1				Repeat 2				Repeat 3			
HA-Gata19	+	+	+	-	+	+	+	-	+	+	+	-
SAP05 (WT)	+	-	-	-	+	-	-	-	+	-	-	-
SAP05 (mut)	-	+	-	+	-	+	-	+	-	+	-	+
Lane	A	B	C	D	E	F	G	H	I	J	K	L
Rel HA/rbcL	0.04	0.89	1.00	0.01	0.01	0.47	1.00	0.00	0.07	0.90	1.00	0.00

	SAP05 N77R											
Leaf	Repeat 1				Repeat 2				Repeat 3			
HA-Gata19	+	+	+	-	+	+	+	-	+	+	+	-
SAP05 (WT)	+	-	-	-	+	-	-	-	+	-	-	-
SAP05 (mut)	-	+	-	+	-	+	-	+	-	+	-	+
Lane	A	B	C	D	E	F	G	H	I	J	K	L
Rel HA/rbcL	0.05	0.02	1.00	0.01	0.12	0.03	1.00	0.04	0.01	0.00	1.00	0.01

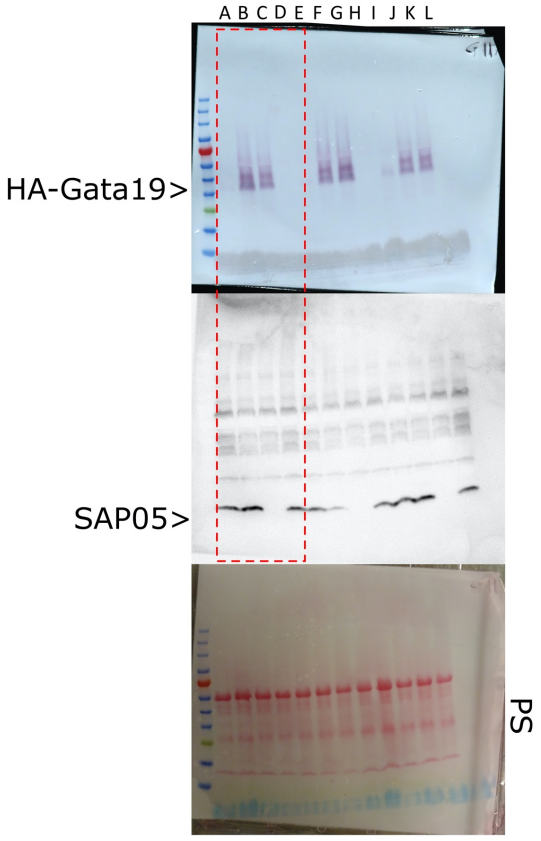

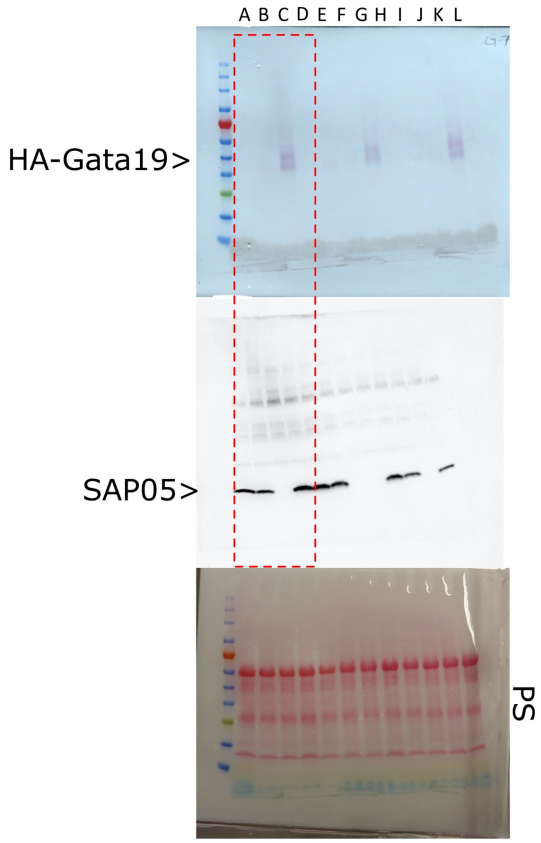

Fig. 3B

The degradation efficiency (Rel HA/rbcL) was calculated as the HA intensity divided by the RuBisCo large subunit (rbcL) intensity from the same sample, then normalized to the coexpression of GFP and HA-SPL5 sample. Red dashed rectangles indicate the cropped image shown in the main figure.

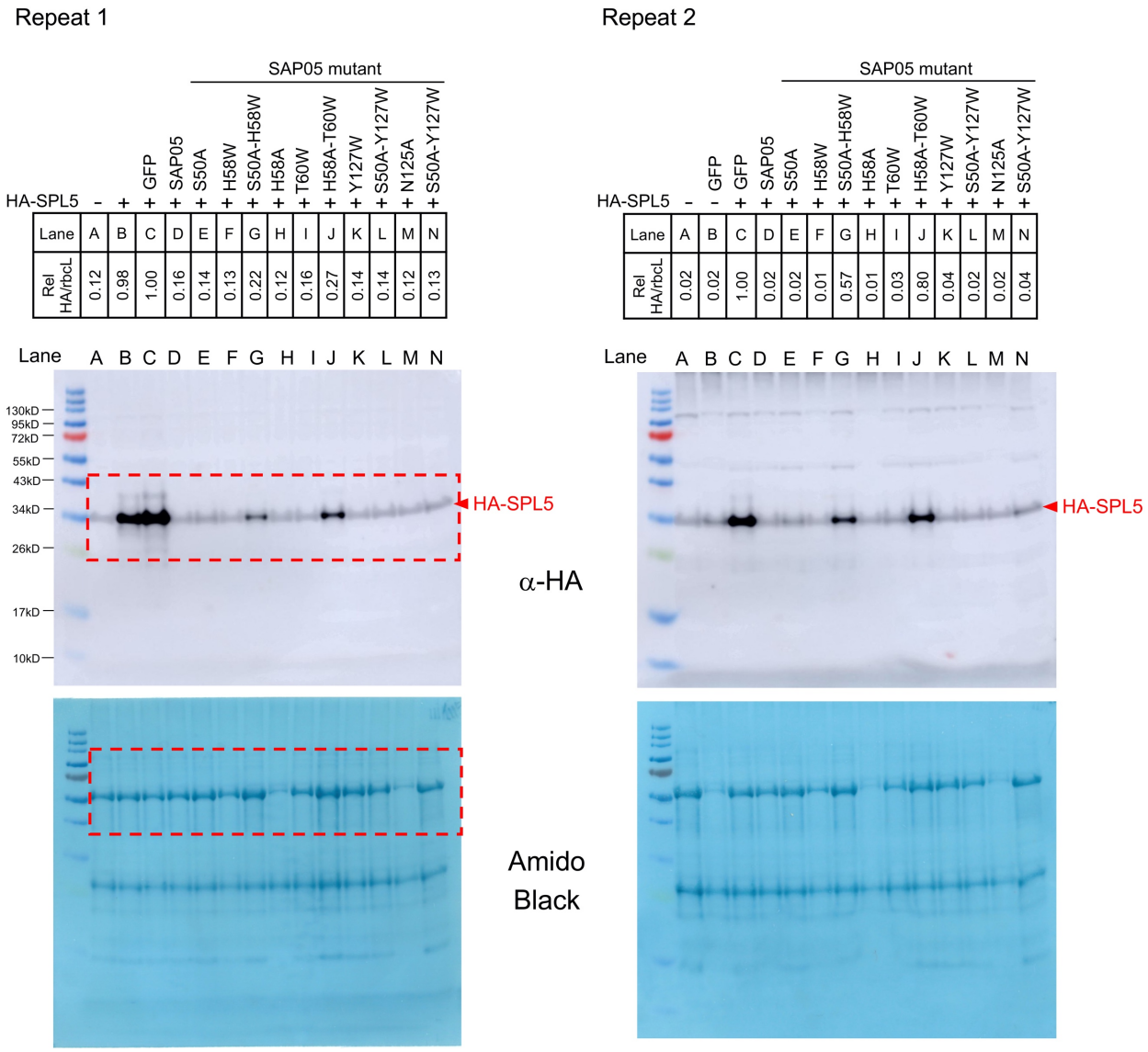

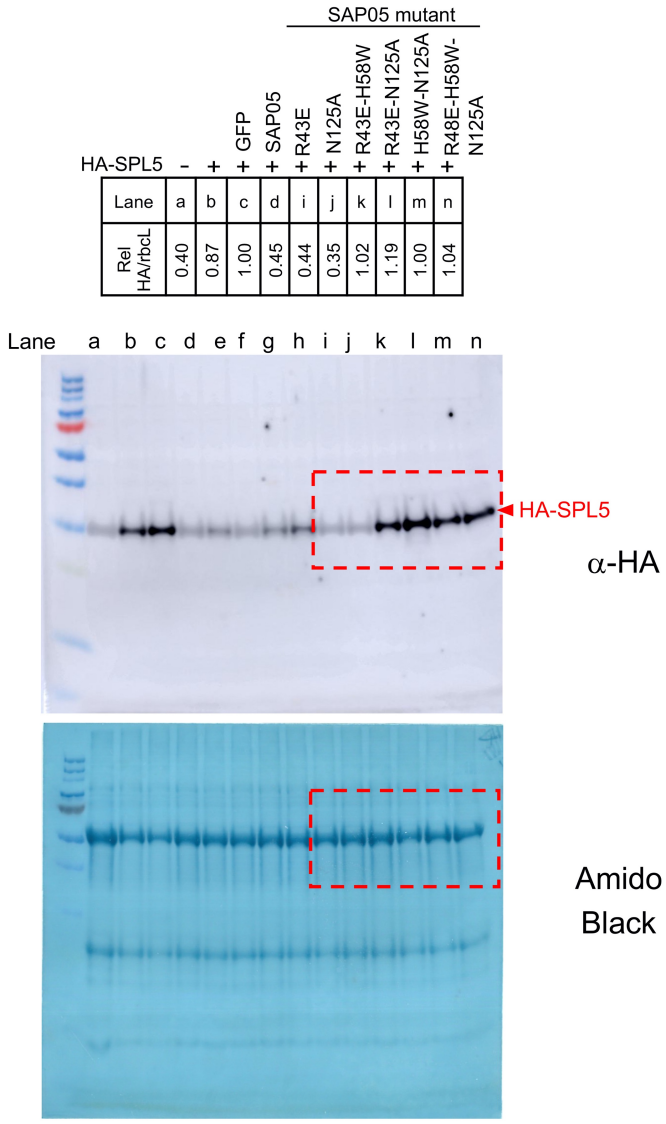
SAP05 mutant
HA-SPL5 – + + GFP + SAP05 + R43E + N125A + R43E-H58W + R43E-N125A + H58W-N125A + R48E-H58W-N125A
Lane a b c d i j k l m n
Rel HA/rbcL 0.40 0.87 1.00 0.45 0.44 0.35 1.02 1.19 1.00 1.04
Lane a b c d e f g h i j k l m n
HA-SPL5
α-HA
Amido Black

SI Appendix Fig. S10

The degradation efficiency (Rel HA/rbcL) was calculated as the HA intensity divided by the RuBisCo large subunit (rbcL) intensity from the same sample, normalized to the intensity of the sample with the highest ratio from the same leaf. The expected size for SAP05, SPL5, and GATA19 is indicated. Experiments included in the main figures are indicated with red dashed rectangles. *Failed experiments due to errors in controls.

	SAP05 R43A											
Leaf	Repeat 1				Repeat 2				Repeat 3			
HA-SPL5	+	+	+	-	+	+	+	-	+	+	+	-
SAP05 (WT)	+	-	-	-	+	-	-	-	+	-	-	-
SAP05 (mut)	-	+	-	+	-	+	-	+	-	+	-	+
Lane	A	B	C	D	E	F	G	H	I	J	K	L
Rel HA/rbcL	0.38	0.28	1.00	0.03	0.47	0.46	1.00	0.03	0.14	0.19	1.00	0.02

	SAP05 R43E											
Leaf	Repeat 1				Repeat 2				Repeat 3			
HA-SPL5	+	+	+	-	+	+	+	-	+	+	+	-
SAP05 (WT)	+	-	-	-	+	-	-	-	+	-	-	-
SAP05 (mut)	-	+	-	+	-	+	-	+	-	+	-	+
Lane	A	B	C	D	E	F	G	H	I	J	K	L
Rel HA/rbcL	0.07	0.21	1.00	0.00	0.13	0.41	1.00	0.01	0.09	0.32	1.00	0.01

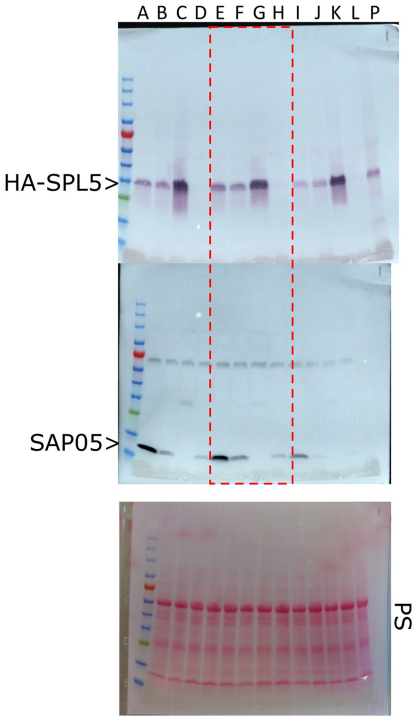

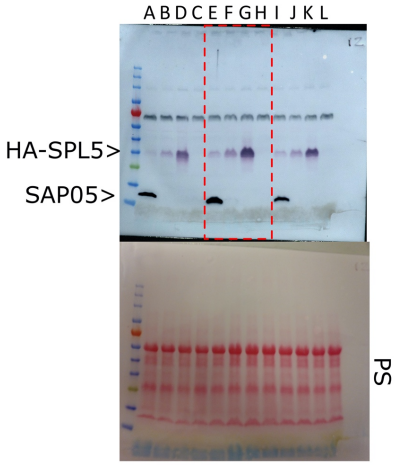

	SAP05 S50A											
Leaf	Repeat 1				Repeat 2*				Repeat 3			
HA-SPL5	+	+	+	-	+	+	+	-	+	+	+	-
SAP05 (WT)	+	-	-	-	+	-	-	-	+	-	-	-
SAP05 (mut)	-	+	-	+	-	+	-	+	-	+	-	+
Lane	A	B	C	D	E	F	G	H	I	J	K	L
Rel HA/rbcL	0.16	0.33	1.00	0.00	1.00	0.59	0.99	0.00	0.43	0.26	1.00	0.00

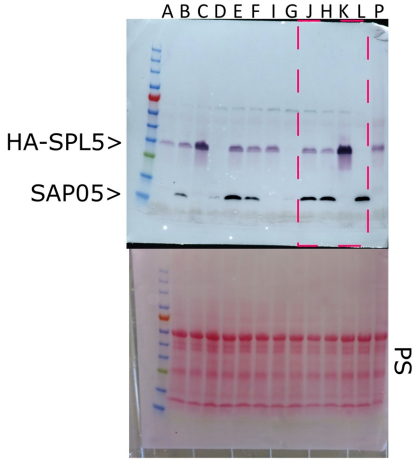

	SAP05 H58A											
Leaf	Repeat 1				Repeat 2				Repeat 3			
HA-SPL5	+	+	+	-	+	+	+	-	+	+	+	-
SAP05 (WT)	+	-	-	-	+	-	-	-	+	-	-	-
SAP05 (mut)	-	+	-	+	-	+	-	+	-	+	-	+
Lane	A	B	C	D	E	F	G	H	I	J	K	L
Rel HA/rbcL	0.55	0.23	1.00	0.01	0.26	0.21	1.00	0.00	0.27	0.19	1.00	0.00

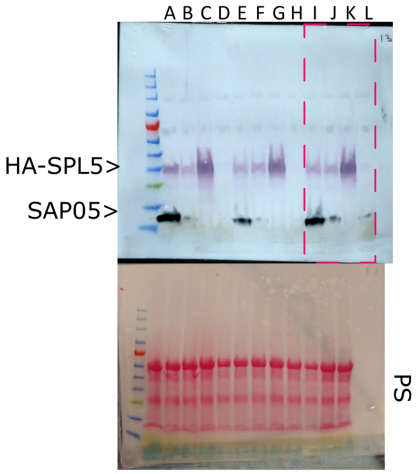

	SAP05 H58W											
Leaf	Repeat 1				Repeat 2*				Repeat 3			
HA-SPL5	+	+	+	-	+	+	+	-	+	+	+	-
SAP05 (WT)	+	-	-	-	+	-	-	-	+	-	-	-
SAP05 (mut)	-	+	-	+	-	+	-	+	-	+	-	+
Lane	A	B	C	D	E	F	G	H	I	J	K	L
Rel HA/rbcL	0.14	0.03	1.00	0.01	1.00	0.14	0.40	0.02	0.15	0.01	1.00	0.00

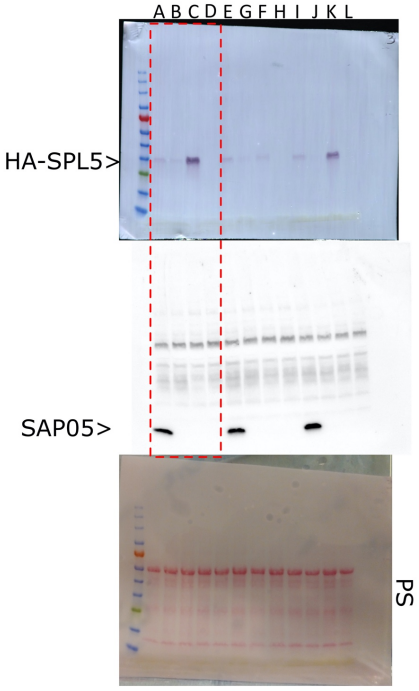

	SAP05 T60W											
Leaf	Repeat 1				Repeat 2				Repeat 3*			
HA-SPL5	+	+	+	-	+	+	+	-	+	+	+	-
SAP05 (WT)	+	-	-	-	+	-	-	-	+	-	-	-
SAP05 (mut)	-	+	-	+	-	+	-	+	-	+	-	+
Lane	A	B	C	D	E	F	G	H	I	J	K	L
Rel HA/rbcL	0.31	0.31	1.00	0.01	0.72	0.31	1.00	0.02	1.00	0.43	0.18	0.02

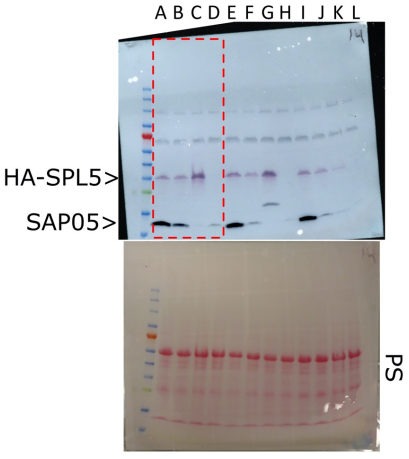

	SAP05 N125A											
Leaf	Repeat 1				Repeat 2*				Repeat 3			
HA-SPL5	+	+	+	-	+	+	+	-	+	+	+	-
SAP05 (WT)	+	-	-	-	+	-	-	-	+	-	-	-
SAP05 (mut)	-	+	-	+	-	+	-	+	-	+	-	+
Lane	A	B	C	D	E	F	G	H	I	J	K	L
Rel HA/rbcL	0.11	0.05	1.00	0.03	1.00	0.17	0.58	0.01	0.25	0.12	1.00	0.01

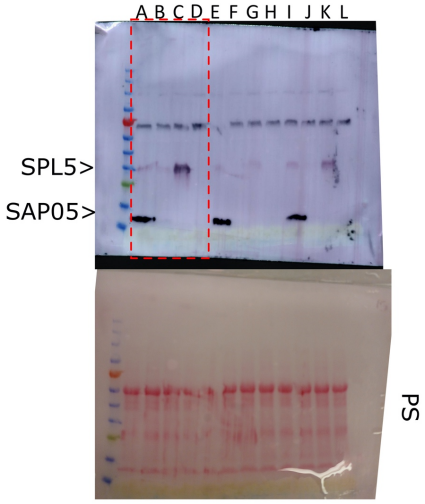

	SAP05 N125D											
Leaf	Repeat 1				Repeat 2				Repeat 3*			
HA-SPL5	+	+	+	-	+	+	+	-	+	+	+	-
SAP05 (WT)	+	-	-	-	+	-	-	-	+	-	-	-
SAP05 (mut)	-	+	-	+	-	+	-	+	-	+	-	+
Lane	A	B	C	D	E	F	G	H	I	J	K	L
Rel HA/rbcL	0.37	0.07	1.00	0.01	0.16	0.03	1.00	0.00	1.00	0.20	0.58	0.03

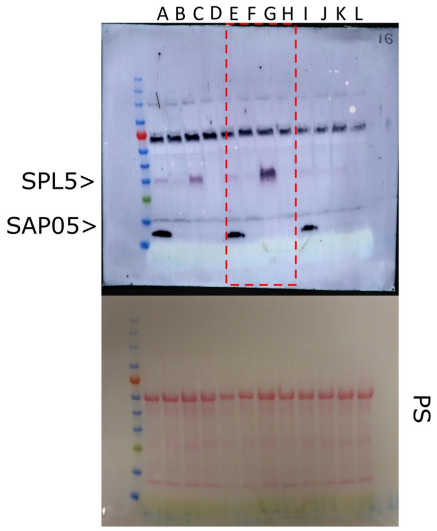

	SAP05 Y127W											
Leaf	Repeat 1				Repeat 2				Repeat 3			
HA-SPL5	+	+	+	-	+	+	+	-	+	+	+	-
SAP05 (WT)	+	-	-	-	+	-	-	-	+	-	-	-
SAP05 (mut)	-	+	-	+	-	+	-	+	-	+	-	+
Lane	A	B	C	D	E	F	G	H	I	J	K	L
Rel HA/rbcL	0.30	0.24	1.00	0.02	0.27	0.26	1.00	0.05	0.15	0.12	1.00	0.01